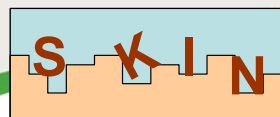




EUROPEAN
COMMISSION

European
Research Area



Final Report

Deliverable D1.5

SLOW PROCESSES IN CLOSE-TO-EQUILIBRIUM CONDITIONS FOR RADIONUCLIDES IN WATER/SOLID SYSTEMS OF RELEVANCE TO NUCLEAR WASTE MANAGEMENT

SKIN

COLLABORATIVE PROJECT (CP)

Grant agreement N°.: FP7-269688

Submitting organizations: ARMINES

Due date of deliverable: Project Month 38

Actual submission: Project Month 39

Start date of the project: 01 January 2011

Duration: 36 months

Project co-funded by the European Commission under the Seventh Framework Programme of the European Atomic Energy Community (Euratom) for nuclear research and training activities (2007 to 2011)

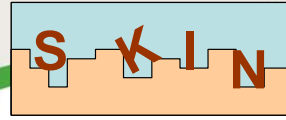
Dissemination Level

PU	Public	×
RE	Restricted to a group specified by the partners of the project	
CO	Confidential, only for partners of the project	



EUROPEAN
COMMISSION

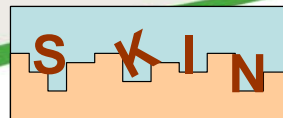
European
Research Area





EUROPEAN
COMMISSION

European
Research Area



FINAL REPORT

Grant Agreement number: 269688

Project acronym: SKIN

Project title: Slow processes in close-to-equilibrium conditions for radionuclides in water/solid systems of relevance to nuclear waste management

Funding Scheme: Collaborative Project

Date of latest version of Annex I against which the assessment will be made: 09/11/2010

Period covered: from 01 / 01 / 2011 **to** 31 / 12 / 2013

Name, title and organisation of the scientific representative of the project's coordinator¹:

Pr. Bernd Grambow, ARMINES / Ecole des Mines de nantes / SUBATECH Laboratory

Tel: +33 251 858 470

Fax: +33 251 858 488

E-mail: grambow@subatech.in2p3.fr

Project website² address:

http://www.emn.fr/z-subatech/skin/index.php/Main_Page

¹ Usually the contact person of the coordinator as specified in Art. 8.1. of the Grant Agreement .

² The home page of the website should contain the generic European flag and the FP7 logo which are available in electronic format at the Europa website (logo of the European flag: http://europa.eu/abc/symbols/emblem/index_en.htm logo of the 7th FP: http://ec.europa.eu/research/fp7/index_en.cfm?pg=logos). The area of activity of the project should also be mentioned.

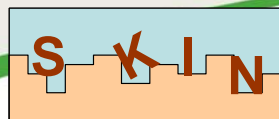
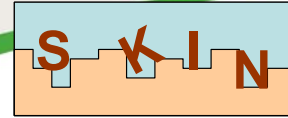


TABLE OF CONTENT

1. FINAL PUBLISHABLE SUMMARY REPORT.....	5
1.1. CONTEXT.....	5
1.2. OBJECTIVES OF THE PROJECT.....	5
1.3. A DESCRIPTION OF THE MAIN S&T RESULTS.....	6
1.3.1. <i>Workpackage 2: Sulfate, Calcite, Cement, Silicates (Lead: D. Bosbach – FZJ)</i>	<i>7</i>
Sulfates (Lead: D. Bosbach (FZJ) / Participants: KIT, FZJ and CTH)).....	9
Carbonates (Lead: F. Heberling (KIT)).....	11
Cements (Lead: N. Evans (LU)).....	13
Silicates (Lead: T. Suzuki-Muresan (SUBATECH/ARMINES))	17
1.3.2. <i>Workpackage 3: Experimental programme on Oxides (Lead: L. Duro –Amphos 21)</i>	<i>18</i>
Interaction of Uranium with Iron(III) oxides (Lead: M. Grivé, E. Colàs, L. Duro (Amphos 21)).....	19
Thorium oxide solubility behavior vs. the surface crystalline state (Lead: J. Vandendorre, T. Suzuki-Muresan (SUBATECH/ARMINES))	21
Study of the dissolution behavior of TcO ₂ (Lead: J. Hinchliff (LU))	23
ThO ₂ /bentonite colloids (Lead: Daqing Cui (SU) and Kastriot Spahiu (SKB))	26
Study of the gamma irradiation on the redox behavior of uranium (Lead: C. Liu (PKU))	27
1.3.3. <i>Workpackage 4: Modelling and Theory (Lead: D. Kulik - PSI)</i>	<i>28</i>
Approaches to model the kinetics of trace element uptake in host minerals (Lead B. Thien, D.A. Kulik, E. Curti (PSI))	29
Modelling the experimental data on radium uptake during barite recrystallization (Lead E. Curti (PSI))	30
Theory on the Affinity Law (Lead S. Ribet, B.Grambow (SUBATECH/ARMINES))	33
1.3.4. <i>Workpackage 5: Synthesis and Safety assessment (Lead: B. Grambow (SUBATECH/ARMINES), L. Duro (AMPHOS 21), K. Spahiu (SKB)).....</i>	<i>35</i>
Overall synthesis.....	35
Impact on safety analyses	40
Future work	45
1.4. THE POTENTIAL IMPACT (INCLUDING THE SOCIO-ECONOMIC IMPACT AND THE WIDER SOCIETAL IMPLICATIONS OF THE PROJECT SO FAR) AND THE MAIN DISSEMINATION ACTIVITIES AND EXPLOITATION OF RESULTS	48



1. Final publishable summary report

1.1. Context

Implementation of geological disposal of radioactive waste requires assessment of relevant processes in the near-field (waste form and engineered barriers) and far-field (host rock and pathways to the biosphere) to allow for development of robust methodologies for performance and safety assessment. Questions need to be answered as to whether the engineered and geological barrier systems can isolate and retain the radionuclides in the waste for hundreds of thousands of years. Relevant processes are all those affecting the mobility of radionuclides.

Due to slow groundwater movement in confined deep geological formations, the system of radionuclides, minerals, engineered barrier materials and water will be close to chemical equilibrium. These systems, controlling radionuclide mobility, have been studied for many years, but only little attention has been given to the fact that, due to the long disposal time, individual very slow processes like surface incorporation of adsorbed substances can have a significant impact on the mobility of radionuclides, despite achievement of local equilibrium states being achieved.

1.2. Objectives of the project

The project has 10 partners, including national waste management organizations, national research centers, universities/grandes écoles and SMEs, from 5 EU Member States (France, Germany, Sweden, Spain, and United Kingdom), one Associated Country (Switzerland), one Other Country (China) and one associate group (Spain).

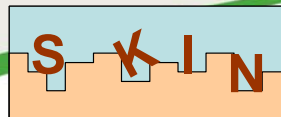


Figure 1-1: Partners involved in SKIN project (number of partners/country)



EUROPEAN
COMMISSION

European
Research Area



The objectives of the project were to study the slow processes influencing radionuclide mobility in close-to-equilibrium scenarios in a detailed and systematic manner in relation to surface properties, surface site detachment/attachment kinetics, irreversible sorption and surface incorporation, for cases relevant to the assessment of radionuclide mobility in nuclear waste repository sites.

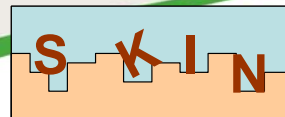
Emphasis was on the temporal evolution of surface detachment and attachment rates on minerals and the coupling of surface equilibrium with slow bulk phase diffusion/recrystallization processes of trace element (incorporation in mineral volume or release). This concerned kinetic studies, thermodynamic evaluations of solid solution/aqueous solution equilibrium, trace and principal element relations, structural and morphological observations and modelling.

The project strategy combined laboratory experiments and model development with analyses of safety consequences of remaining uncertainties. The work consisted in combining, for relevant time frames, bottom-up approaches with individual mineral/water systems with top-down analyses of performance assessment needs to describe non-linearly coupled exchange processes in geological disposal environments. The work programme covered various experimental case studies for solubility and sorption equilibria combined with surface incorporation and associated model development of practical relevance for application within performance assessment.

1.3. A description of the main S&T results

The work program of SKIN was structured along 4 RTD work packages (WP2-5, Figure 1-2). They covered near-field and far-field aspects to assess the slow processes close-to-equilibrium which results have been implemented in Performance Assessment/Safety Case.

- Experimental programs have been performed in WP2 and WP3: WP2 focused on the formation and on slow processes close-to-equilibrium of solid solutions in aqueous environments under waste repository near-field and far-field aspects as well as cement-related systems; WP3 focused on the understanding of the kinetics of alteration of oxides from primary solids, as well as the secondary solid phases expected to form under repository conditions after the eventual release of the radionuclides present in the different waste.
- WP4 has assessed the experimental results by geochemical thermodynamic modelling and its new partial-equilibrium approach and by the affinity law and its validity close to equilibrium.



- WP5 has performed a synthesis of results of experimental, modelling and safety assessment approaches in the context of a full assessment of the literature, and inclusion of literature data.

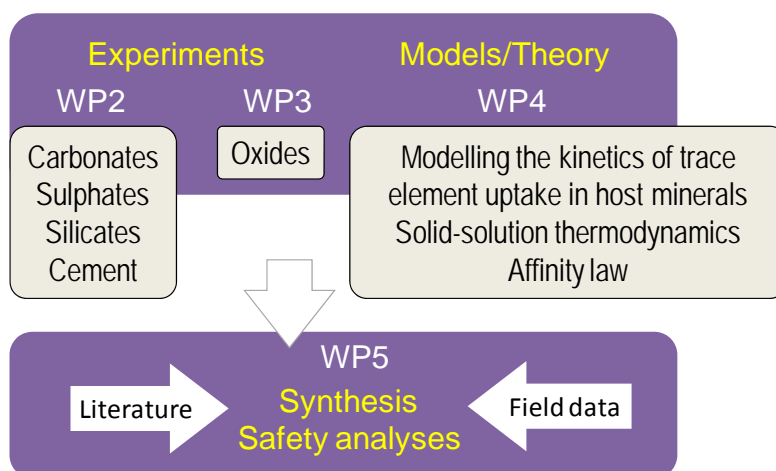


Figure 1-2: Organisation des workpackage RTD

Activities and main results have been overviewed by each workpackage leader. Each task leader has also reported the main important results obtained during the final period of the project.

1.3.1. Workpackage 2: Sulfate, Calcite, Cement, Silicates (Lead: D. Bosbach – FZJ)

WP2 addresses the formation and slow processes close-to equilibrium of solid solutions in aqueous environments under waste repository near-field and far-field aspects as well as cement related systems. Five different partners worked together within this working package: Karlsruhe Institute of Technology (KIT) worked on carbonates. Forschungszentrum Jülich (FZJ), KIT and Chalmers University of Technology (CHT) together worked on sulfates. ARMINES worked on clays and Loughborough University (LU) on cements.

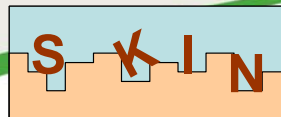
The following tasks were studied in detail:

- The applicability of $Ra_xBa_{1-x}SO_4$ solid solution - aqueous solution thermodynamics to a specific disposal scenario
- The reversibility of solid/solution interaction with clays



EUROPEAN
COMMISSION

European
Research Area



- Identification of the substitution scheme for complex metal ion substitutions: calcite and selenite
- Identification of metal ion binding - precipitation, co-precipitation, surface uptake - in complex cement related systems

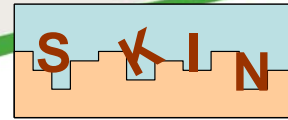
Within the time frame of SKIN, barite completely recrystallizes to a $Ra_xBa_{1-x}SO_4$ solid solution – which can now be thermodynamically described based on the available data obtained within SKIN from recrystallization experiments, solubility studies and EXAFS data.

The results obtained for the illite/smectite system indicate that in conditions close to equilibrium a dynamic exchange of ^{29}Si and ^{28}Si occurs at the interface solid/solution. XPS and XRD analyses indicate no modification for both initial and altered illite/smectite after alteration. The ratios of Al/Si for initial and altered illite/smectite as well as for initial and altered Callovo-Oxfordian argillite confirm only weak changes of the chemical environment of Si and Al as a function of temperature and alteration time.

With respect to the interaction of selenite with calcite, the new results indicate that selenite adsorption on the calcite surface and selenite coprecipitation with calcite under supersaturated conditions can be described with the same partition coefficient – thus implying that the coprecipitation in this case may be viewed as a sequence of adsorption and entrapment events. Furthermore, the interactions of selected radionuclides (Cm, Eu, Np) or their none-radioactive analogues with various carbonate minerals was studied.

Within the SKIN project methods were developed to investigate the diffusion, advection and incorporation of Ca, Sr, Eu, Am and Se isotopes along with HTO in Nirex Reference Vault Backfill (NRVB) and a 3:1 PFA:OPC waste packaging grout. ^{241}Am , ^{152}Eu and ^{75}Se could not be mobilised under the experimental conditions used. The ^{45}Ca results indicate a strong interaction with the NRVB which is most likely due to a combination of isotope exchange and solubility limitation. ^{90}Sr is observed to be more mobile than ^{45}Ca and has a less significant interaction with the solid matrix.

In the following, the main results of each task of WP2 are summarized.



Sulfates (Lead: D. Bosbach (FZJ) / Participants: KIT, FZJ and CTH)

Context of the study

Within WP 2.1 Ra uptake experiments, thermodynamic calculations, structural analysis of the RaSO_4 endmember and complementary coprecipitation experiments were carried out to gain a deeper understanding of the Ra - BaSO_4 exchange process. A special focus of the Ra uptake experiments is the incorporation of radium into barite, the radio-barite recrystallization mechanism, the solid-solution composition and the ^{226}Ra uptake rate as function of environmental conditions. The results of this working package were provided to WP 4 to support the assessment of safety margins (milestone M2.3). In addition, EXAFS and X-ray powder diffraction was performed to gain detailed structural information about the RaSO_4 end-member.

^{226}Ra uptake experiments

A combined macroscopic and microanalytical approach was applied in order to distinguish between two possible scenarios for the uptake of ^{226}Ra by already existent barite under repository relevant conditions: (1) formation of a $\text{Ba}_{1-x}\text{Ra}_x\text{SO}_4$ solid solution surface layer on the barite or (2) a complete recrystallization, leading to homogenous $\text{Ba}_{1-x}\text{Ra}_x\text{SO}_4$ crystals.

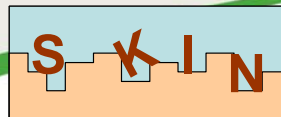
The ^{226}Ra uptake by barite at ambient conditions and 90 °C was studied in in long-term batch experiments (> 800 days). Recrystallization experiments were carried out for two different types of barite with different initial surface areas and an initial ^{226}Ra concentration of $5 \cdot 10^{-6}$ mol/L. The results obtained at ambient conditions show a significant decrease of more than 99 % of the ^{226}Ra concentration in the presence of barite. Both with 0.5 g/L and 5 g/L, the ^{226}Ra decreases in several steps to a minimum concentration before it slowly approaches a steady state. The final steady state ^{226}Ra concentrations after 800 days at ambient conditions can well be described with the interaction $a_0 = 1.0$ and a RaSO_4 solubility product $\log K_{\text{SP}}(\text{RaSO}_4) = -10.26$, corresponding to recently published theoretical results for the interaction parameter and the solubility product of RaSO_4 described in the NAGRA-PSI database. At 90 °C ^{226}Ra uptake into barite during batch recrystallization experiments is significantly lower than at room temperature. This was explained quantitatively by the variation of the end-member solubilities at RT and 90 °C as calculated with GEM-Selektor code. The results of this task were used in WP 4 for detailed kinetic and thermodynamic modelling.

ToF-SIMS results show that all barite particles analyzed within this study contain Ra not only on their surfaces but within the grains. For most grains, a homogenous distribution of Ra could be determined, indicating complete recrystallization of barite into a $\text{Ba}_{1-x}\text{Ra}_x\text{SO}_4$.



EUROPEAN
COMMISSION

European
Research Area



From the intensities of ^{226}Ra and Ba obtained during the ToF-SIMS, $^{226}\text{Ra}/\text{Ba}$ intensity ratio distributions were computed. The maximum of the histogram is identical with the expected $^{226}\text{Ra}/\text{Ba}$ ratio calculated from mass balance under the assumption of complete recrystallization.

In summary, two different effects of the presence of ^{226}Ra can be observed, depending on the original PSD. The wide PSD of a fine grained barite is significantly altered during the recrystallization of barite in the presence of ^{226}Ra compared to a Ra free reference. On the other hand, the particle size of a coarse grained barite sample with a narrow PSD remains more or less constant. Here, eventually a coarsening due to the presence of Ra is expected due to the formation of new grains from intergrown agglomerates.

Combined ^{223}Ra and ^{133}Ba uptake experiments

The study of the kinetics of $^{223}\text{Ra}/^{133}\text{Ba}$ recrystallization on the surface of synthesized BaSO_4 crystals has been studied. The use of short-lived ^{223}Ra isotope (half-life 11.4 days) allows reaching concentrations below 10^{-13} M as found in natural water environments. The concentrations of $^{223}\text{Ra}^{2+}$ and $^{133}\text{Ba}^{2+}$ spikes are far below the calculated solubility of corresponding RaSO_4 and BaSO_4 . The addition of the second $^{223}\text{Ra}^{2+}$ spike after 42 days allows to detect a mechanism of recrystallization, *i.e.* while ^{223}Ra concentration of the second spike decreases, $^{133}\text{Ba}^{2+}$ concentration (no additional barium added) first, increases before it starts to decrease again. It was found that the system follows the homogeneous recrystallization model and that recrystallization rates, inferred by the decrease of ^{223}Ra and ^{133}Ba in the aqueous solution, are fast.

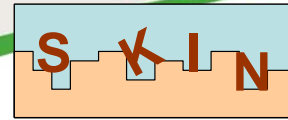
Properties of the RaSO_4 -end-member

The RaSO_4 structure studies using XRD and, for the first time, EXAFS showed that it belongs to orthorhombic space group and is isostructural with BaSO_4 and SrSO_4 . The unit cell parameters of RaSO_4 were determined to be orthorhombic, belonging to the Pnma (No. 62) space group with the cell parameters $a = 9.07 \text{ \AA}$, $b = 5.52 \text{ \AA}$, $c = 7.28 \text{ \AA}$ and $V = 364.48 \text{ \AA}^3$. The bond distances were determined using EXAFS. The mean Ra-O and S-O bond distances were found to be $2.96(2) \text{ \AA}$ and $1.485(8) \text{ \AA}$ respectively and the Ra-O-S bond angle was $127(2)^\circ$. These data were consistent with and supported by the XRD data. These findings indicate that it may be possible for Ra to co-precipitate with BaSO_4 , SrSO_4 and PbSO_4 to form a substitution solid solution. In addition, the solubility of RaSO_4 was studied at room temperature and elevated temperatures.



EUROPEAN
COMMISSION

European
Research Area



Coprecipitation of Sr, Ba and Ra sulfates

The experimental results show that it is possible for Ra to co-precipitate with Ba, Sr and Pb in sulphate media to form a substitutional solid solution. The activation energy for the precipitation of the pure sulfates decreases in the order $Sr > Ba > Ra$, which may be correlated to their ionic size, since this affects the ability to lose their hydration water. The activation energy (E_a) is lower for the precipitation of pure $RaSO_4$ than for $RaSO_4 - BaSO_4$. The activation energy for $RaSO_4 - BaSO_4$ is closer to the one determined for pure $RaSO_4$. This means that the temperature dependence is less for the precipitation of $RaSO_4$ than $BaSO_4$, this is also true for the $RaSO_4 - BaSO_4$ solid solution, when comparing to pure barite.

Carbonates (Lead: F. Heberling (KIT))

Context of the study

In the multi-barrier system around a nuclear waste repository, carbonate minerals have the potential to sequester radionuclides released from the waste, by adsorption and structural incorporation reactions, and to keep them from migrating towards the biosphere. The aim of Task 2.2 was to study the interactions of selected radionuclides (Se/ Cm/ Eu/ Np) or their non-radioactive analogues with some carbonate minerals (calcite/ aragonite/ strontianite). Batch type dissolution, adsorption, or recrystallization experiments, or mixed flow reactor (MFR) crystal growth experiments were used to investigate these interactions as a function of supersaturation. Spectroscopic (TRLFS/ EXAFS) and microscopic (AFM, SEM) methods were applied in order to get insight into the reaction mechanisms involved. Final goal of the studies is to develop thermodynamic models which can be used to predict the radionuclide behavior in the geosphere.

Se(VI/IV)-calcite

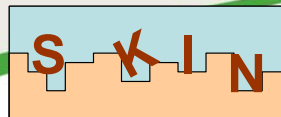
Se(VI) showed no significant interaction with calcite in MFR experiments, in zeta potential measurements, as well as in AFM in-situ calcite dissolution experiments.

In similar AFM dissolution experiments in the presence of Se(IV), a significantly increased etch pit formation was observed. At high pH Se(IV) causes a decrease of calcite zeta potential. MFR experiments conducted over a large range of Se(IV) concentrations ($10^{-13} - 10^{-4}$ M) at low supersaturation, indicate a linear increase of the SeO_3^{2-}/CO_3^{2-} ratio in the solid with the increase of the SeO_3^{2-}/CO_3^{2-} ratio in the contact solution. The structure of the incorporated species was investigated using Se K-edge EXAFS. These investigations confirmed the structural incorporation of selenite into calcite by the substitution of carbonate for selenite, leading to the formation of a $Ca(SeO_3)_x(CO_3)_{(1-x)}$ solid solution. The linear



EUROPEAN
COMMISSION

European
Research Area

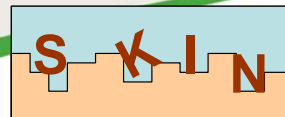


relationship between $\text{SeO}_3^{2-}/\text{CO}_3^{2-}$ ratio in solution and in the solid can be described under the assumption of an ideal mixing between calcite and a virtual CaSeO_3 end member, whose standard Gibbs free energy ($G^0(\text{CaSeO}_3_{\text{exp}}) = -953 \pm 6 \text{ kJ/mol}$, $\log_{10}(K_{\text{SP}}(\text{CaSeO}_3_{\text{exp}})) = -6.7 \pm 1.0$) is defined by linear extrapolation of the excess free energy from the dilute Henry's law domain to $X(\text{CaSeO}_3) = 1$. In contrast to this experimental result, DFT and force field calculations predict the virtual bulk CaSeO_3 end member to be significantly less stable and more soluble: $G^0(\text{CaSeO}_3_{\text{bulk}}) = -912 \pm 10 \text{ kJ/mol}$ and $\log_{10}(K_{\text{SP}}(\text{CaSeO}_3_{\text{bulk}})) = 0.5 \pm 1.7$. To explain this discrepancy a thermodynamic adsorption/entrapment concept was introduced. This concept is based on the idea that the experimental value of $-953 \pm 6 \text{ kJ/mol}$ reflects the Gibbs free energy of CaSeO_3 within the surface layer, while the value obtained by atomistic calculations reflects bulk thermodynamic properties. In coprecipitation experiments the difference in Gibbs free energy between these values is compensated by affinity due to supersaturation. Thus, if the Gibbs free energies of the bulk CaCO_3 and CaSeO_3 end members are substituted with the Gibbs free energies of the surface end members, the coprecipitation experiment can still be treated within the formalism of equilibrium thermodynamics. This concept leads to a number of important consequences, which were tested both experimentally and theoretically. We showed that selenite adsorption at the calcite surface and selenite coprecipitation with calcite under supersaturated conditions can be described with the same partition coefficient. This implies that the coprecipitation can be viewed as a sequence of adsorption and entrapment events. On the other hand, aragonite recrystallization experiments showed that at near equilibrium conditions calcite growth is inhibited in the presence of selenite. Consistently with these observations, DFT calculations showed that the substitution of carbonate for selenite is energetically more favourable at the surface than inside the bulk.

The whole set of the experimental and atomistic simulation results leads to the conclusion that the calcite- CaSeO_3 solid solution can only grow continuously if the aqueous solution is supersaturated with respect to the bulk solid solution. Under these conditions selenite coprecipitates with calcite at a partition coefficient of $D = 0.02 \pm 0.01$. If the solution is undersaturated with respect to the bulk solid solution, only surface ion-exchange occurs. Elevated selenite concentrations in bulk calcite therefore reflect non-equilibrium conditions.

Eu(III)/Cm(III) – strontianite/ celestite

In previous studies it was shown that trivalent lanthanides and actinides show a very high affinity for incorporation into carbonate minerals (calcite/aragonite/vaterite), while incorporation into sulfate minerals (gypsum) is very limited. Aim of the investigation was to use the isostructural carbonate and sulfate minerals strontianite (SrCO_3) and celestite (SrSO_4) in order to assess whether preferred incorporation into carbonates is an effect of the structure



or an effect of the ligand field. It could be shown by TRLFS that Eu(III) and Cm(III) are structurally incorporated into both mineral phases. However, the partition coefficient for incorporation into strontianite is orders of magnitude higher than that for incorporation into celestite. This emphasizes the effect of the ligand field on incorporation affinity.

Eu(III)-calcite/aragonite

Eu(III) shows a very high affinity for the incorporation into aragonite. Even in batch type adsorption experiments the main part of Eu(III) is incorporated into aragonite within 24 hours. The empirical partition coefficient for incorporation $D = 200$. As aragonite is thermodynamically less stable than calcite, aragonite dissolves in aqueous solution in favor of the formation of the more stable phase, calcite. In the presence of Eu(III) at high solid to liquid ratio ($S/L = 20$ g/L) a large part of the Eu(III) in aragonite is incorporated into calcite upon recrystallization. TRLFS revealed that the speciation of Eu(III) in calcite obtained by aragonite recrystallization is different from the speciation of Eu(III) in calcite obtained in previous calcite coprecipitation experiments. At low solid to liquid ratio ($S/L = 0.2$ g/L) the presence of $1 \mu\text{mol/L}$ Eu(III) in solution stabilized aragonite against recrystallization to calcite. This sets constraints to the thermodynamics of the Eu-aragonite and Eu-calcite solid solutions. A consistent thermodynamic description of the experiments is, however, not yet possible.

Np(V)-calcite

Neptunium(V) can be structurally incorporated into calcite upon coprecipitation. Np(V) adsorbs at steps at the calcite surface and strongly decreases the calcite growth rate in Np(V) coprecipitation experiments. Within SKIN two sets of aragonite to calcite recrystallization experiments in the presence of $1 \mu\text{mol/L}$ Np(V) were launched. One in 0.1 mol/L NaCl and the other in 0.1 mol/L KCl, in order to assess whether the alkali metal cation plays a role in charge compensation upon substitution of NpO_2^+ for Ca^{2+} . The experiments are still running. First results are available, but not yet conclusive.

Cements (Lead: N. Evans (LU))

Context of the study

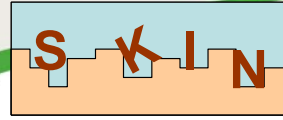
Cementitious media may serve a variety of purposes in Geological Disposal Facilities (GDF) for Intermediate Level Waste (ILW), including waste packaging and backfill.

The aim was to develop methods to investigate the diffusion, advection and incorporation of Ca, Sr, Eu, Am and Se isotopes along with HTO in Nirex Reference Vault Backfill (NRVB) and a 3:1 PFA:OPC waste packaging grout. Diffusion and advection experiments were



EUROPEAN
COMMISSION

European
Research Area



undertaken with the objective of characterising the ability of the selected cementitious media to contain or retard the migration of the selected radioisotopes. Techniques were developed and data relevant to the kinetics and thermodynamics of the processes were collected. Initial GoldSim modelling of the diffusion data using a 1D simplification of the radial geometry yielded diffusivities and partition coefficients comparable with literature values. It was also possible to run the experiments in the presence and absence of cellulose degradation products (CDP) and observe the impact of these organics on radioisotope mobility. All experiments were undertaken in the absence of carbon dioxide and the fate of the isotopes ascertained using gamma spectroscopy, autoradiography and XRD.

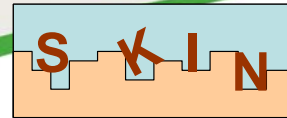
Radial Diffusion Technique

The experimental method for diffusion was developed during the first year of work. The technique uses the radial migration of the isotopes through cylinders of the cementitious media. The diffusion apparatus is illustrated below. The cylinder dimensions were ~45 mm height and 40 mm diameter.



Figure 1-3: Schematic and photograph of diffusion apparatus

The inner core where the radioisotopes are added was 10 mm diameter and ~30 mm deep. The top and bottom surfaces of the cylinders were sealed with wax. As the radioisotope migrates through the cylinder side walls and into the surrounding water the increase in concentration can be monitored by sampling. The method was found to be suitable for NRVB and the waste packaging grout and therefore assumed to be suitable for the porous cements, backfills and grouts likely to be used in GDF engineering. It was also found to be suitable for tracer only and tracer carrier experiments provided the isotope is mobile at the high pH values involved. In this series of experiments it was possible to acquire data for HTO, ^{90}Sr and ^{45}Ca . However,



^{241}Am , ^{152}Eu and ^{75}Se were found to be immobile across the available duration of the experiments.

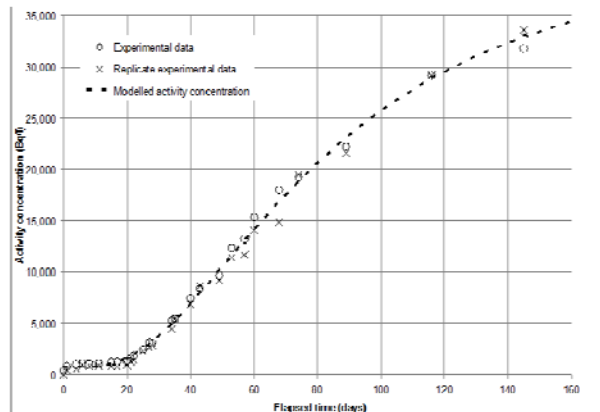


Figure 1-4: A typical set of results from the diffusion experiments undertaken using ^{90}Sr and NRVB. The hashed line is the modelled result and the o and x represent the results of the duplicates. It can be seen that the results are reproducible and readily modelled using the 1D simplification of the radial geometry

Radial Advection Technique

The advection apparatus uses the same sample geometry but a cell was designed and manufactured that allows the fluid to be pushed through the central core and collected as it exits the outer surface of the cementitious material. The advecting fluid can be pumped from a reservoir under nitrogen pressure eliminating the need for operation in a glove-box. A modified gas chromatography injector was used to facilitate the injection of the radioisotopes directly into the central core.

Successful experiments with ^{90}Sr , ^{45}Ca and HTO in the presence and absence of CDP have been completed.



EUROPEAN
COMMISSION

European
Research Area

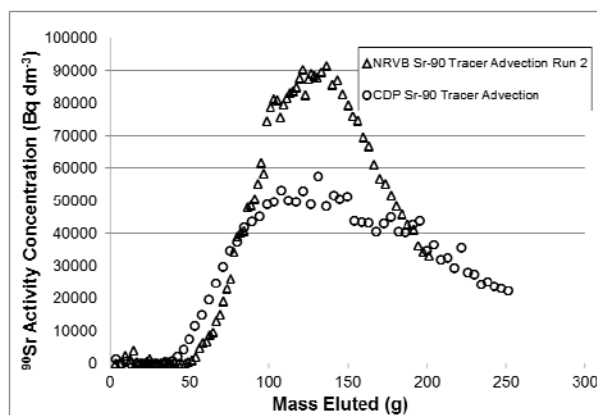
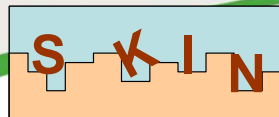
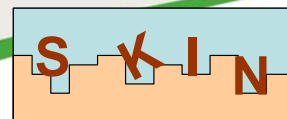


Figure 1-5: A typical set of results from the advection experiments undertaken using ^{90}Sr and NRVB, Two runs are shown one in the presence of CDP and the other in the absence of CDP. A clear difference in the elution profiles can be seen. The CDP appears to be slowing down the tracer elution and increasing its dispersion. The method produced repeatable results but the GoldSim model could not applied with complete success.

Conclusions

The diffusion and advection experiments have shown that there are clear differences in mobility between the radionuclides tested. ^{241}Am , ^{152}Eu and ^{75}Se could not be mobilised under the experimental conditions used. The comparison between ^{90}Sr and ^{45}Ca is significant. The ^{45}Ca results indicate a strong interaction with the NRVB which is most likely due to a combination of isotope exchange and solubility limitation. The ^{45}Ca results in the presence of CDP may indicate that precipitation/dissolution of an organic Ca salt is the dominant effect. Additional work will be required to confirm this. The ^{90}Sr results indicate that it is more mobile than ^{45}Ca and has a less significant interaction with the solid matrix.



Silicates (Lead: T. Suzuki-Muresan (SUBATECH/ARMINES))

Context of the study

According to the French laws for the management of nuclear wastes, high level nuclear glass wastes are planned to be stored in the Callovo-Oxfordian geological formation. Dissolution rates of nuclear waste glass are known to depend strongly on dissolved silica concentrations. The question raised in the SKIN project was how the surface of the Callovo-Oxfordian argillite will behave in presence of a source term in silicon stemming from the radioactive nuclear glass waste. For that, two clay minerals (illite and interstratified illite/smectite) considered as reference minerals were studied and compared to the Callovo-Oxfordian argillite at different temperatures. The work was focused on the close to equilibrium conditions and the assessment of the surface reactivity was performed by the $^{29}\text{Si}/^{28}\text{Si}$ isotopic exchange.

Experimental results

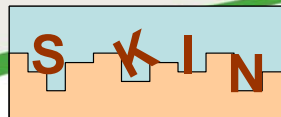
Natural clayey samples used for this project was illite/smectite ISCz1 and illite IMT2 provided by Clay Mineral Society (C.M.S.), and Callovo-Oxfordian argillite from the Underground Research Laboratory at Bure. The experiments were performed in batch systems at 35 °, 50 ° and 90 °C. The solution composition was NaCl 0.01 mol/L with an initial pH of 5.5. The stable isotope of silicon ^{29}Si was used to study the isotopic exchange between ^{28}Si and ^{29}Si at the interface solid/solution. Dissolution rates and precipitation rates were calculated after addition of ^{29}Si spike according to the quantity of Si released from clayey minerals, and the precipitation rates have been calculated by considering the quantity of ^{29}Si -spike remained in solution. Maximum concentration of Si values ($\sim 10^{-5} - \sim 10^{-4}$ mol/L) was reached after 50 days of contact time. These values lower than the solubility values of quartz may correspond to the solubility of the clays. As far as solution concentration controls of dissolved silica are concerned, the data indicates that the influence of the quartz fraction contained in the clayey materials can be neglected in this study. Concentration of Fe is 2.5×10^{-6} mol/L and Al is 3×10^{-6} mol/L in solution with a strong influence of temperature on the release rates and on the maximum concentration in solution.

After 326 - 483 days of alteration, a ^{29}Si spike was added in each system studied. The results obtained for the illite/smectite system indicate that in condition close to equilibrium a dynamic exchange of ^{29}Si and ^{28}Si occurs at the interface solid/solution. The isotopic exchange was performed during 100 days with a dissolution rate of $\sim 7 \times 10^{-15}$ mol Si/m²/s and a precipitation rate of $\sim 4 \times 10^{-15}$ mol Si/m²/s. This indicates an exchange of Si between solid surface and the solution. It also means that the isotopic ratio $^{29}\text{Si}/^{28}\text{Si}$ at the surface has



EUROPEAN
COMMISSION

European
Research Area



reached a new value different from the bulk solid. If this isotopic exchange continues beyond the exchange of surface atoms (in case of clay of Si atoms at edge sites) the exchange ratio will very slowly to evolve towards the reference value of natural $^{29}\text{Si}/^{28}\text{Si}$ isotopic ratio. The rate of the change in isotopic ratios will then indicate the extent of recrystallization of the minerals. About 36 % (35 ° and 50 °C) and 20 % (90 °C) of Si have been exchanged between illite/smectite and solution and half of this quantity has been exchanged after 18 days.

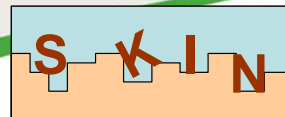
XPS and XRD analyses indicate no modification for both initial and altered illite/smectite after 538 days of alteration. XRD analyses showed no structural modifications after 640 days of experiments. Ratio of Al/Si was calculated from the quantitative data obtained by XPS. The results at 35°, 50° and 90°C give a ratio of 0.36 for both initial and altered illite/smectite, of 0.34 for both initial and altered illite, and of 0.30 for both initial and altered Callovo-Oxfordian argillite. This value is in good agreement with the literature data confirming the weak change of the chemical environment of Si and Al against the temperature and the alteration duration.

1.3.2. Workpackage 3: Experimental programme on Oxides (Lead: L. Duro – Amphos 21)

The global objective of this WP is the assessment of the dissolution processes of oxides of relevance for the safety assessment of the repository in close to equilibrium conditions. To this aim, the following specific investigations were defined from the onset of the project:

- Study of the nature and long term kinetics of the interaction between actinides and major near field components, linking short-term sorption and long-term coprecipitation processes and their study through specific solid spectroscopy.
- Study of the kinetics of dissolution of tetravalent oxides under conditions close to equilibrium, with special focus on the study of the solid-liquid interface, including monitoring of the composition of the surface through isotopic exchange techniques.
- Study of the effect of near field materials on the kinetics of dissolution of tetravalent oxides and the potential of bentonite colloids as drivers for dissolution enhancement.

6 Different partners work within this workpackage: ARMINES, Loughborough University (LU) Stockholm University (SU) and SKB work on the study of the dissolution of tetravalent actinides under quasi equilibrium conditions. To this aim, ARMINES works with ThO_2 , LU works with TcO_2 , and SU and SKB work with UO_2 and with ThO_2 as a proxy for UO_2 in order to avoid unwanted oxidation of UO_2 to U(VI). Amphos 21, SU and the University of



Beijing (PKU) work on the influence of major systems present in the repository on the rate of dissolution of matrix-related material and the retention/release of radionuclides.

In the following sections, a brief summary of the work performed within each one of the individual activities is presented.

Interaction of Uranium with Iron(III) oxides (Lead: M. Grivé, E. Colàs, L. Duro (Amphos 21))

Iron oxides are the main products of canister corrosion and can be present among the engineered and geological barriers. Among the iron oxides, the amorphous ferrihydrite is one of the most widespread iron solids and an important precursor of more stable and crystalline iron oxides. Ferrihydrite evolution with time and the final products formed depend on many factors, such as pH, time, temperature, etc. The presence of foreign species (such as uranium) in the system will affect the ferrihydrite ageing process. The ageing and transformation process of ferrihydrite will affect in turn the solubility and the retention/release process of uranium from the coprecipitates.

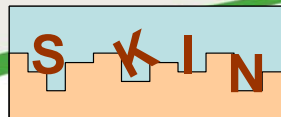
The objectives of this task have been:

1. To assess which is the effect of U on the aging process of ferrihydrite
2. To assess which is the effect of the aging process of ferrihydrite on the retention/mobility of U
3. To assess which is the influence and the role of carbonates in the overall process?

To this aim, several experimental techniques used in the study include both specific solid spectroscopy techniques and conventional solution chemistry techniques.

U(VI)-Fe(III) coprecipitates were prepared by alkaline co-precipitation of U(VI) ($\approx 1-2\%$) with Fe(III) homogeneous solutions. Samples were aged at room temperature (under N_2 atmosphere or in the presence of carbonate, in contact with atmospheric $CO_2(g)$) in aqueous solutions at different time intervals, from days to 5 weeks. Additional samples were stored under dry conditions and aged for several years. In addition, samples where uranium was sorbed onto ferrihydrite at different ageing times and in the presence and the absence of CO_2 were also prepared. The samples were analyzed using conventional solution techniques and several spectroscopic techniques: X-ray diffraction (XRD), Extended X-Ray-absorption Fine Structure (EXAFS) and micro- X-ray fluorescence (μ -XRF).

According to the XRD analysis of the samples aged at 3 weeks and 9 years, the bulk of U(VI)-Fe(III) coprecipitates can be assumed to evolve from a 2L ferrihydrite to a 6L



ferrihydrate-like. The results obtained in the EXAFS (Fe K-edge) measurements were consistent with the XRD results. The results obtained in the EXAFS (U L_{III}-edge) measurements are consistent with an edge-sharing bond between U(VI) and ferrihydrate. Those results also indicate that the bonding environment of uranium in the coprecipitates evolves with ageing time, towards a schoepite-like structure. The conclusion obtained from that observations indicate that the U(VI)-Fe(III) coprecipitate has a ferrihydrate-like structure which evolves in the ageing process. Uranium measurements are consistent with a re-arranging of the uranium content towards a schoepite-like structure. This would imply that the assessment of the efficiency of this retention process at long time frames would be given by the schoepite solubility limit.

The results obtained from μ -XRF indicate interesting correlations between Fe and U. The samples are heterogeneous and a clear correlation between Fe and U content and a regrouping of uranium as the coprecipitate ages is observed, as shown in the figure below:

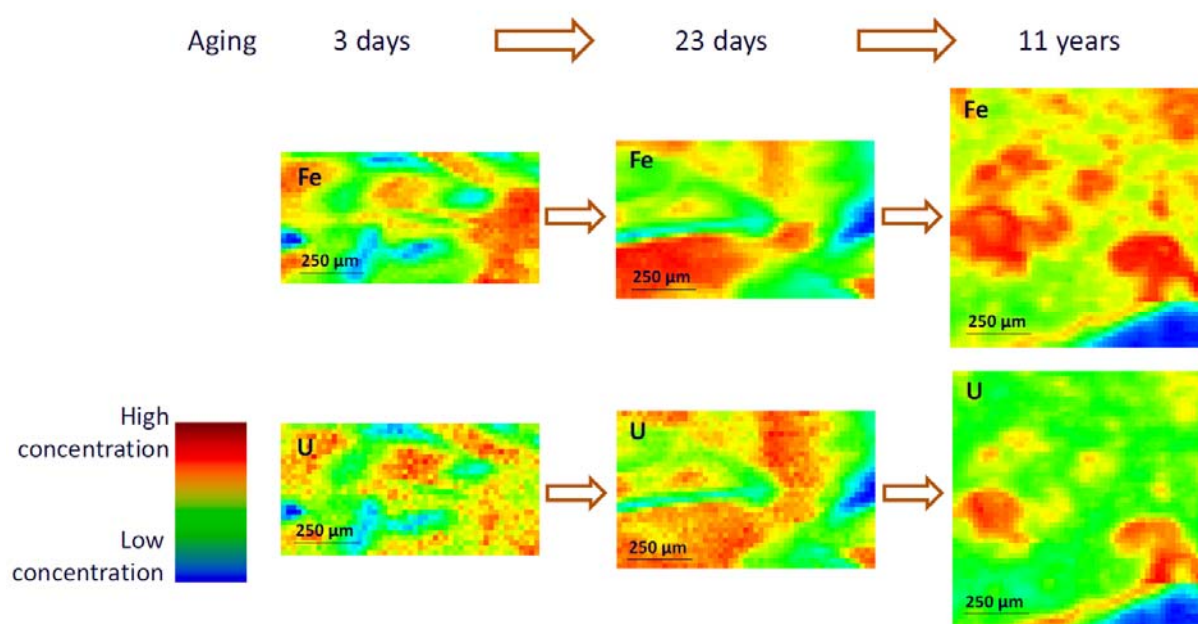
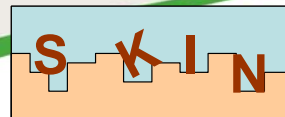


Figure 1-6: μ -XRF mapping of U and Fe for samples of different aging times showing the correlations between uranium and iron enriched areas.

The dissolution process of ferrihydrate, schoepite and the Fe(III)-U(VI) coprecipitate was shown to be affected by carbonate; the results obtained point out a bicarbonate promoted dissolution of the three solids. The dissolution rates have a linear dependence with the



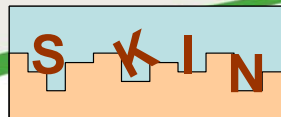
logarithm of bicarbonate concentration, and the rate equations for the dissolution of each solid on bicarbonate solutions were determined. The dissolution process of the coprecipitate by effect of the carbonate ligand appeared to be a non-congruent dissolution process, where uranium dissolves preferentially than iron.

Thorium oxide solubility behavior vs. the surface crystalline state (Lead: J. Vandenborre, T. Suzuki-Muresan (SUBATECH/ARMINES))

In literature, huge discrepancies are reported in solubility values and it is now accepted that the surface solid state may have influence on the determination of the solubility values. The aim of the work in SKIN-project was to re-assess the solubility of $\text{ThO}_2(\text{s})$ in the pH range 3 to 7 as a function of the surface crystalline state.

Previous studies indicated that thorium oxide solubility is dependent on the material at the grain boundary. With the use of powdered material, the cleaning of the surface is expected to be more effective, so that artefacts derived from pre-altered surface phases will be minimised. We studied Th atom exchange between different thorium oxide surfaces and aqueous solution (0.01 mol.L^{-1} NaCl for pH = 3.2, 5.0, 6.8) to address Task 3.2. Therefore for sparingly soluble solids, one needs to quantify the specific surface site involved in the attachment and detachment rates if one wants to assess solubility constraints. For this reason, the purpose of our work was to assess different crystalline states of thorium oxide surfaces with different grains vs. grain boundaries ratios. In this aim, we synthesized thorium oxides from thorium oxalate $\text{Th}(\text{C}_2\text{O}_4)_2 \cdot 4 \text{H}_2\text{O}$ as precursor in order to control the grain size of ThO_2 crystallized with different heating temperatures ($T = 700^\circ\text{C}$, 900°C , 1300°C). The second solid used in this study is under spherical particles forms and synthesized at a high calcination temperature (1600°C). A part of the spheres used for solubility experiments are crushed in order to remove all the grain boundaries even into the core of the sphere by the pre-washing experiments. We obtain the 4 sets of solid sample: (I) Crushed ThO_2 spheres, (II) Initial ThO_2 spheres, (III) ThO_2 powder synthesized at 1300°C , (IV) ThO_2 powder synthesized at 700°C .

SEM picture of HTR sphere surface shows grains of ThO_2 coated by grain boundaries which control the solubility without pre-washing. The solids characterization by XRD is performed onto the ThO_2 spheres in order to check the high crystalline state of this sample. From the results, we confirm the different crystallization states by the decrease of Full Width Half Middle observed onto the XRD peaks when the heating temperature increases. Hence, the ratio between grains and grain boundaries is different for all these samples. The B.E.T. method give us the specific surface area values between $17.8 \text{ m}^2/\text{g}$ for the lower crystallized sample (synthesized at 700°C) and $1.9 \text{ m}^2/\text{g}$ for the higher crystallized (synthesized at



1300°C). The specific area value for initial ThO₂ sphere can be estimated from the geometric structure at $1.2 \cdot 10^{-3} \text{ m}^2/\text{g}$.

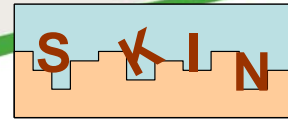
The attainment of apparent solubility equilibrium was followed by analysing ²³²Th with time. In condition close to equilibrium, half of the solution was removed and kept for desorption experiment. In the remaining half solution in the experiments, ²²⁹Th trace was added to the solution/solid system and the isotopic exchange was monitored. Once ²²⁹Th uptake on the surface has reached a steady state, desorption experiments was performed putting the solids with a ²²⁹Th enriched surface into the previously conserved solution without ²²⁹Th. The relative enrichment in ²²⁹Th is a parameter linked to the solubility of a solid surface and is calculated by the ratio between two ratios of ²²⁹Th onto ²³²Th at the surface and at the solution. Typical duration of experiments is longer than a year (> 500 days). These results indicate the similar behaviour and the close crystalline degree between the powder synthesized at 1300°C (III) and the crushed sphere (I). It seems that the global and the kinetic dissolution behaviours are similar for these two samples. From the results, we made the evidence that the crystalline state of the samples is involved in the dissolution mechanism during the initial kinetic leaching and the reaching of the pseudo steady-state equilibrium. The normalized mass loss rates (NLR) depending on the specific surface area show again the similar behaviour between the powder synthesized at 1300°C (III) and the crushed sphere (I). Finally the same evolution of the ratios grain/grains boundaries and global/kinetic leaching behaviour can be described as following: (IV) > (II) > (I) = (III). Then, after the ²²⁹Th addition, a quick precipitation of the ThO_x(OH)_y(H₂O)_z phase occurs at the surface of the ThO₂ powder synthesized at 700°C (I) and the slow leaching of this phase is following by the ²²⁹Th and ²³²Th isotopes measurements.

Relative enrichment (RE) values in ²²⁹Th have been calculated for each sample. These calculations check that all sample surfaces are more and more rich in ²²⁹Th isotope because RE increases with contact time and is high than 1. The RE values of samples IV, 700°C powder, and II, initial sphere, quickly increase for the first days of contact time after ²²⁹Th addition (between 200 and 250 days) which correspond to the precipitation process of the ThO_x(OH)_y(H₂O)_z phase in grain boundaries (GB) for the Initial sphere case. For the second part of contact time (between 300 and 450 days) a steady-state is measured for all the samples with for higher than 10 RE values (samples IV and II with GB) a dynamic isotopic exchange between the surface and the solution; and for the other samples (I and III without GB) with RE values lower than 10 a pseudo equilibrium state with no Th isotopes exchange between the surface and the solution. For the last part (between 450 and 550 days of contact time) no change in RE values occurs for the samples (I and III) without GB because of the slow



EUROPEAN
COMMISSION

European
Research Area

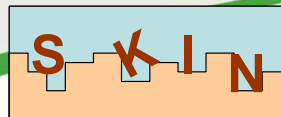


dissolution process of the ThO_2 crystallized grains ($5 < \text{RE} < 10$). Moreover, no change occurs too for the samples IV (700°C powder) due to the thermodynamic solubility equilibrium reached for this system by the main $\text{ThO}_x(\text{OH})_y(\text{H}_2\text{O})_z$ phase control with an high RE value ($300 < \text{RE} < 400$). However, for the Initial sphere (sample II) the same behaviour than for the first part is observed but it is relied on the redissolution process of the $\text{ThO}_x(\text{OH})_y(\text{H}_2\text{O})_z$ phase into the GB with RE value close to the sample IV (~ 100).

We have described the different behaviour of the surfaces of ThO_2 versus the surface crystalline state. The use of the isotopic $^{229}\text{Th}/^{232}\text{Th}$ exchange assesses the key issue of this Workpackage: the realistic solubility behaviour of the ThO_2 surface. We have classified the 4 sets of solid samples versus the leaching behaviour: (IV) > (II) > (I) = (III) with (I) Crushed ThO_2 spheres, (II) Initial ThO_2 spheres, (III) ThO_2 powder synthesized at 1300°C, (IV) ThO_2 powder synthesized at 700°C. Moreover, the behavior of the solid versus the $^{229}\text{Th}/^{232}\text{Th}$ exchange occurs if the $\text{ThO}_x(\text{OH})_y(\text{H}_2\text{O})_z$ phase is implied into the solid surface leaching. Moreover, three kinds of surfaces of the ThO_2 have been studied: (1) Powder synthesized at low temperature (700°C): this surface displays a low crystallinity with a strong control of the thermodynamic solubility by the $\text{ThO}_x(\text{OH})_y(\text{H}_2\text{O})_z$ phase. The curve of relative enrichment in ^{229}Th isotope vs. the contact time gives the high exchange between the surface and the solution in order to reach this thermodynamic equilibrium ; (2) Initial HTR sphere of ThO_2 : this surface presents a high crystallinity but with grain boundaries (GB). In this case it is the accessibility of the GB phase, probably the same phase that $\text{ThO}_x(\text{OH})_y(\text{H}_2\text{O})_z$, which control the dissolution/precipitation/redissolution mechanisms. These processes have been check by SEM analysis where the grains size of ThO_2 clearly evolves during the contact time. The curve of relative enrichment in ^{229}Th isotope vs. the contact time makes the evidence that the high slope value of the RE corresponds to the precipitation process and for the second one to the redissolution process of the GB phase; (3) Powder synthesized at high temperature (1300°C) and the crushed HTR sphere: these both samples present exactly the same behavior for all the 500 days of solid/solution contact experiment. These surfaces present a high crystallinity without GB. The main process is the slow dissolution of the ThO_2 crystallized grains which is validated by the slow evolution of the RE curve slope. In this case, the thermodynamic solubility cannot be reached before a higher contact time than in our study (500 days).

Study of the dissolution behavior of TcO_2 (Lead: J. Hinchliff (LU))

The UK presents a high inventory of ^{99}Tc in the wastes to manage. Under the expected GDF conditions of high pH and low Eh most technetium should be immobile as the solid phase TcO_2 (am). Nevertheless, not much is known about the behaviour of this solid phase, which is



the reason why this task focused on the study of TcO_2 solubility and evolution with time in the high pH range at different ionic strengths.

To this aim, high purity $\text{TcO}_2(\text{s})$ was produced electrochemically and a proportion left to age for 12 months, although experiments commence on the freshly produced $\text{TcO}_2(\text{s})$. Different experimental set ups were used:

1. Study of the dissolution of TcO_2 under fresh solutions
2. Study of the dissolution of TcO_2 under undisturbed conditions

For the two setups, fully-reduced, high purity $^{99}\text{TcO}_2(\text{s})$ was produced electrochemically using the method in Warwick *et al* (*Radiochimica Acta*, 2007, 95(12), 709-716), from ammonium pertechnetate. The ammonium pertechnetate solution (20 mL in a 50 mL centrifuge tube, concentration $4 \times 10^{-6} \text{ mol L}^{-1}$ technetium in each tube) was adjusted to pH 10.5, 12.5 or 13.3 and ionic strength 1.0 mol L^{-1} or 3.0 mol L^{-1} in a nitrogen atmosphere anaerobic glove box ($< 1 \text{ ppm O}_2$), before reduction for 2 hours at a potential difference of 6 V using a vitreous carbon cathode and Pt wire anode in the presence of 0.01 mol L^{-1} sodium dithionite as a holding reductant. Three replicates of each system were set-up and kept in an anaerobic glove box for up to 12 months for sampling. To investigate the effect of the age of the solid phase the systems were centrifuged and the supernatant removed to waste.

In the case of the “fresh-solution experiments”, the solution in contact with the solid was replaced by an equal volume of the same solution, i.e., the same pH and ionic strength. The new system was allowed to equilibrate for 24 hours before a sample was taken in triplicate for measurement of the aqueous concentration of technetium.

In the case of the “undisturbed conditions”, the solution in contact with the solid was not replaced after sampling, but was left to evolve with time.

For the “fresh-solution experiments”, the results obtained showed no correlation between the age of the solid phase and the measured aqueous concentration in the supernatant after 24 hours equilibration. Higher concentrations were measured in those experiments conducted under higher ionic strengths (3M NaCl). Increasing pH resulted in an increase of the Tc concentration in solution for the experiments at $I=3\text{M}$, while for those at $I=1\text{M}$, the effect of pH increase on Tc concentrations is only noticeable in the higher pH range, when changing from 12.5 to 13.3. The experimental data are plotted in Figure 1-7.

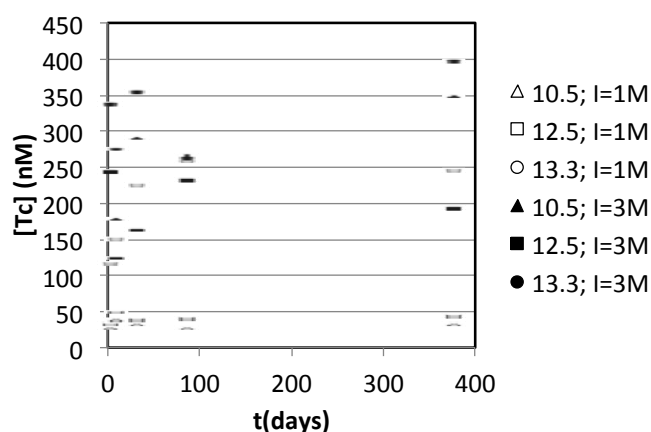
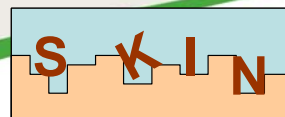
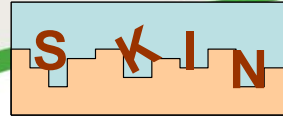


Figure 1-7: Concentration of Tc in solution for the experiments conducted under fresh solutions at different ionic strength and pH. Open symbols stand for the lower and solid symbols for the higher ionic strength.

For the six different systems investigated a comparison is shown in Table 1-1 between the ‘steady-state’ and ‘fresh solution’ measured aqueous concentrations of technetium. In 3 cases there is a statistically significant difference, at pH 10.5 – I = 1.0 mol L⁻¹, at pH 10.5 – I = 3.0 mol L⁻¹ and at pH 12.5 – I = 3.0 mol L⁻¹. In each case the measured ‘fresh solution’ concentration of technetium was significantly the higher.

Table 1-1. Comparison of ‘Fresh Solution’ and ‘Steady-State’ supernatant concentrations of ⁹⁹Tc from pH 10.5 to 13.3 at ionic strengths of 1.0 and 3.0 mol L⁻¹, errors ± 1 s.d.

pH	Ionic Strength	“Steady-State” [Tc]	“Fresh Solution” [Tc]	Difference significant at 95%?
	(mol L ⁻¹)	(nmol L ⁻¹)	(nmol L ⁻¹)	
10.5	1.0	12.8 ± 1.0	22.6 ± 4.7	Yes
10.5	3.0	17.0 ± 2.1	257 ± 63	Yes
12.5	1.0	29.6 ± 3.1	32.2 ± 6.3	No
12.5	3.0	30.3 ± 2.7	182 ± 50	Yes
13.3	1.0	175 ± 33	191 ± 62	No
13.3	3.0	356 ± 59*	316 ± 56	No



ThO₂/bentonite colloids (Lead: Daqing Cui (SU) and Kastriot Spahiu (SKB))

During a glacial period it has been shown that dilute glacial water may cause erosion of the bentonite clay, followed by severe bentonite losses. When the anoxic glacial melt water reaches the repository, the buffer may be partially or completely eroded, leaving a cavity filled with a slurry of colloidal clay particles. These colloidal clay particles are produced through the erosion of the clay in the tunnel backfill. For a canister breached under such circumstances, the clay particles are not expected to affect the fuel oxidative dissolution rate. Dissolved U(IV) would, however, be expected to be sorbed strongly to the clay particles and the amounts of U(IV) sorbed are expected to be proportional to its concentration in solution, that is determined by the solubility of UO₂(s) in case solubility equilibrium is attained. In case the dissolution rate of UO₂(s) is very low, solubility equilibrium will not be attained during the residence time of the clay particles in the canister and the amount adsorbed and transported away will be lower.

Erosion of bentonite in tunnel poses fuel in contact with clay slurry. The amount of uranium transported by bentonite particles is described by equation (1):

$$R_U = [U]_{sol} \cdot q \cdot (1 + C_{clay} \cdot K_d) \quad (1)$$

where: q is the flow rate, C_{clay} - clay concentration and $[U]_{sol}$ - solubility of U(IV).

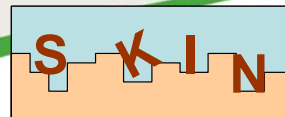
A basic assumption of Equation (1) is U dissolution rate from SNF is not so much slower than U sorption on clay, $[U] \approx [U]_{sol}$, the amount U dissolved from SNF and transport via clay slurry should be much faster than the conditions without clay slurry.

If UO₂ dissolution rate is much lower the U(IV) sorption rate, $[U] \ll [U]_{sol}$ the amount U dissolved from SNF and transport via clay slurry should be much smaller than that at the conditions with near constant solubility level, as assumed in Equation 1.

The transport rate of clay slurry is another important factor. The high clay transport rate may result in the increase of the amount of U sorbed on the clay and that dissolved from SNF.

Because of the difficulties in avoiding oxidation while working with UO₂(s), crystalline ThO₂(cr) was used to simulate the fuel UO₂(s) matrix.

The major objective of this work was to investigate in how much degree the presence of clay slurry can affect the Th(IV) concentration in ThO₂ leaching experiment. This information is useful to predict the migration of radionuclides from SNF repository.



From the results obtained, it can be summarized that $\text{UO}_2(\text{s})$ dissolution rate can be sufficiently low, so that $\text{U}(\text{IV})$ solubility, in the canister void, cannot be satisfied during the time of the residence of the clay slurry in the canister void. In this case, the amount of $\text{U}(\text{IV})$ sorbed on clay particles (proportional to sorption coefficient (K_d) and concentration of $\text{U}(\text{IV})$ in solution) will be lower than that in a solution with the $\text{U}(\text{IV})$ concentration at UO_2 solubility level.

Therefore it can be expected that $[\text{U}](\text{t})$ should be lower or much lower than $[\text{U}](\text{solubility of } \text{UO}_2)$ in a very long period of time, even longer than the time of clay staying in SNF canister void. Therefore, we can conclude that the invasion of clay slurry to canister void during the glacial period can enhance the radionuclide migration, but not so much as that conservatively assumed before (Equation 1, SKBTR-11-01), because the U concentration in the canister void is lower than that in clay slurry free conditions.

Therefore, we can say that it is not fair to calculate the amount of transported $\text{U}(\text{IV})$ by Equation 1 given in the introduction part. This information is useful for the safety assessment.

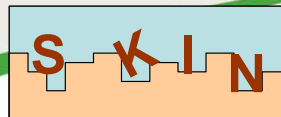
Study of the gamma irradiation on the redox behavior of uranium (Lead: C. Liu (PKU))

The purpose of our work is to study the influence of gamma irradiation on the redox of uranium, and the sorption of uranium oxides on the surface of Beishan Granite under the geological repository conditions. The concentration of uranium (VI) in solution was determined by the Arsenazo III method. During this process, it was found that for ordinary aqueous samples, due to the strong complexing ability, $\text{Fe}(\text{III})$ can significantly decrease the UV-Vis absorbance of the $\text{U}(\text{VI})$ -arsenazo III complex, whereas the influence of $\text{Fe}(\text{II})$ on the absorbance is negligible.

However, when $\text{Fe}(\text{II})$ is present in a gamma-irradiated $\text{U}(\text{VI})$ aqueous sample, it can give rise to the Fenton reaction, which produces oxidative radicals that decompose the subsequently added arsenazo III, leading to a sharp decrease in the absorbance of the $\text{U}(\text{VI})$ -arsenazo III complex. The decrease in absorbance is iron content- and irradiation dose-dependent.

The oxidative radicals from the Fenton reaction induced by gamma irradiation can be continually produced for more than one month in the absence of light under atmospheric conditions, and the reactivity of the radicals had no discernible change towards the subsequently added arsenazo III.

The results of this investigations were submitted as a manuscript "Influence of gamma irradiation on uranium determination with arsenazo III in the presence of $\text{Fe}(\text{II})/\text{Fe}(\text{III})$ " to



CHEMOSPHERE. The article is accepted and in the publication process. The Figure 1-8 shows the graphical abstract of the result.

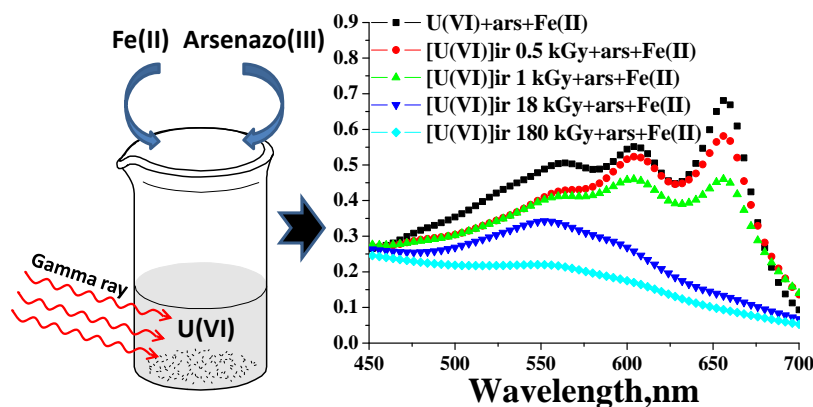


Figure 1-8: The absorbance of pre-gamma irradiated U(VI) solution plus Arsenazo III and Fe(II) as a function of absorbed dose in the range of 0–180 kGy, $[\text{Fe(II)}]_{\text{add}} = 0.1 \text{ mM}$

1.3.3. Workpackage 4: Modelling and Theory (Lead: D. Kulik - PSI)

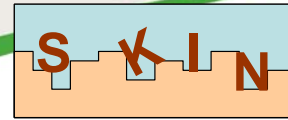
Our studies provide advanced, practical tools for modelling non-equilibrium entrapment of trace radionuclides in solid-solution phases. In particular, the UUKM implementation in the GEM-Selektor code will ultimately allow modelling slow kinetic processes even in complex geochemical systems coupled with transport of reactive chemical species (task 4.1). The results of Ra-barite interaction experiments (task 4.2) impressively demonstrate that kinetic effects may well extend over years, before equilibrium conditions are approached. Neglecting such effects in geochemical models of reactive transport is likely to produce biased results. We believe that slow kinetic processes will need to be further explored in the future (both on the experimental and modelling side) in order to provide safe predictions on the fate of radionuclides in geological repository systems. The objectives of this workpackage were:

- 4.1. To review existing models of time-dependent trace element uptake in host minerals; To find a generalized approach suitable for implementation in geochemical modelling codes; To perform initial tests of routines implementing this approach in the GEM-Selektor code.
- 4.2. To collaborate with partners involved in WP2 Task 2.1, in order to interpret experimental data on barite recrystallization kinetics and on the uptake of radium in the barite structure.
- 4.3. To review the literature data for some typical mineral rates expressed as function of the chemical affinity.



EUROPEAN
COMMISSION

European
Research Area



Approaches to model the kinetics of trace element uptake in host minerals (Lead B. Thien, D.A. Kulik, E. Curti (PSI))

In nuclear waste repositories, the interaction of groundwater with waste packages and host rock may lead to formation of secondary minerals such as carbonate- and sulfate solid solutions. This process is an efficient uptake and retention mechanism for many trace radionuclide elements. The measurable uptake of a given trace element Tr in a host mineral (e.g. calcite) made of element Hc is expressed by a fractionation coefficient $\Delta_{Tr,Hc} = \frac{([Tr]/[Hc])_{mineral}}{([Tr]/[Hc])_{aqueous}}$,

where $[]$ denotes concentration in the appropriate scale (e.g. mole fraction in the mineral, molar in aqueous solution). Equilibrium fractionation coefficients $\Delta_{Tr,Hc,eq}$ can be predicted using a thermodynamic aqueous solid-solution model. However, many studies showed that for a growing host mineral, the experimentally measured $\Delta_{Tr,Hc}$ can be very different from $\Delta_{Tr,Hc,eq}$, resulting in stronger or weaker long-term retention.

Hence, thermodynamics alone may not be sufficient to predict growth-rate dependencies of trace element uptake in host mineral solid solutions. In this study, two uptake kinetic models promising in terms of mechanistic understanding and potential for implementation in geochemical modelling codes have been compared. The Growth Surface Entrapment Model by Watson (2004) and the Surface Reaction Kinetic Model by DePaolo (2011) were shown to be complementary. Under certain assumptions, they were merged into a single analytical expression of the “Unified Uptake Kinetics Model” (UUKM), further implemented in the in-house GEM-Selektor code package for geochemical modelling by Gibbs energy minimization (<http://gems.web.psi.ch>). In turn, this extends the uptake kinetic models to account for the non-trivial impacts on the trace element partitioning into solid solutions, such as changes in aqueous solution composition and speciation, or depletion effects in closed systems.

The UUKM implementation has been tested on the literature data on trace cation co-precipitation kinetics in calcite $CaCO_3$ (Figure 1-9), and on some new experimental data from WP2 for selenite incorporation during fast co-precipitation with calcite.

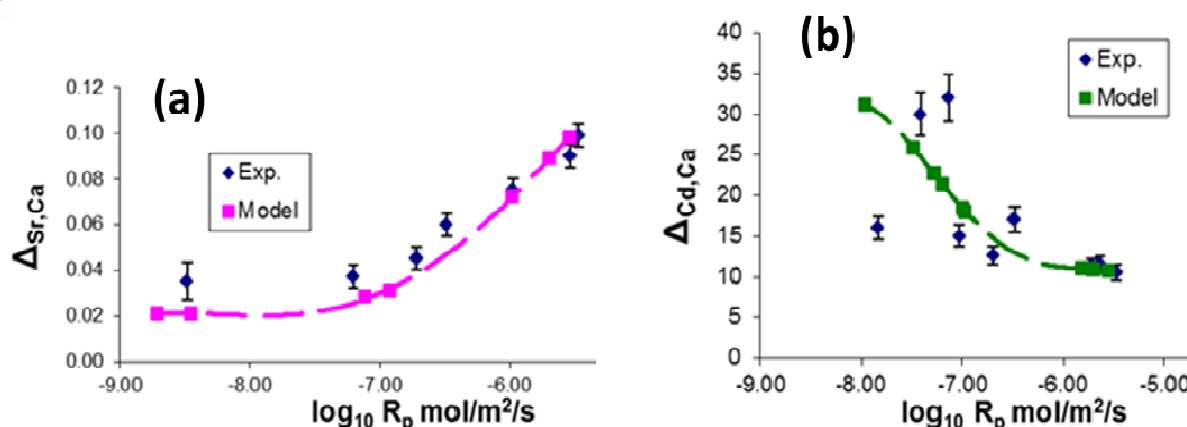
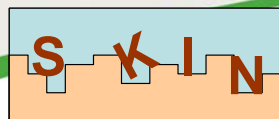
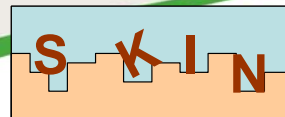


Figure 1-9: Fractionation coefficient as a function of precipitation rate R_p for Sr in calcite (a) and Cd in calcite (b). Curves: our UUKM calculations using the GEM-Selektor code; scattered symbols are experimental data from the literature.

The slower the precipitation rate the more $\Delta_{Tr,Hc}$ tends to $\Delta_{Tr,Hc,eq}$; the higher the precipitation rate the more $\Delta_{Tr,Hc}$ tends to $\Delta_{Tr,Hc,ads}$ - a value corresponding to Tr adsorption on the calcite surface. In particular, strontium Sr with its relatively weak equilibrium incorporation is considered “incompatible” relatively to calcite structure due to its much greater ionic radius than that of calcium. In this case, kinetic effects enhance Sr uptake (Figure 1-9, a), showing that equilibrium thermodynamics alone may under-evaluate the real uptake of “incompatible elements” by factor 3 to 5. On the contrary, cadmium Cd is a “compatible element” in the calcite structure, with high equilibrium incorporation. In this case, kinetic effects decrease the uptake by factor of 2 to 3 (Figure 1-9,b), pointing out that equilibrium thermodynamic models may over-predict the uptake of “compatible elements”. In the context of radioactive waste disposal, the model can now be applied to many Tr/Hc couples of interest in very complex chemical systems involving depletion effects in pores and changes in aqueous speciation.

Modelling the experimental data on radium uptake during barite recrystallization (Lead E. Curti (PSI))

It is well known that the formation of solid solutions leads to a decrease in the equilibrium aqueous concentration of trace elements. This effect could be particularly beneficial to the safety of nuclear waste sites whenever safety-relevant nuclides released from radioactive waste form dilute solid solutions with major host minerals occurring in the near-field of such repositories. Under such circumstances, radionuclide solubility limits may be strongly reduced compared to the solubility control by pure solids. In the case of radium, the formation



of solid solutions with barite $(\text{Ra,Ba})\text{SO}_4$ by the reaction of sulphate solutions with Ba isotopes released from spent fuel or vitrified radioactive waste is considered to be likely. This process would reduce the concentration and thus the mobility of dissolved radium by orders of magnitude compared to the case of solubility control by pure radium sulphate. Eventually, the ^{226}Ra contribution to radiological doses could decrease to levels largely below those predicted assuming that a pure solid (e.g. RaSO_4) controls Ra solubility. Hence, thorough understanding of the mechanisms leading to Ra-barite formation, with careful quantification of related thermodynamic data (non-ideality parameters, end-member solubility products) are the prerequisites to reliably predict the contribution of ^{226}Ra to radiological doses in safety assessment calculations.

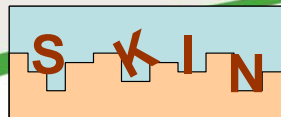
In this task, the main objective was to model the experimental data provided by SKIN partners on the uptake of Ra during barite recrystallization, both in terms of solid solution thermodynamics (determination of interaction parameters) and kinetics (growth rates of Ra-barites). In the framework of the resources granted for this task, it has not been possible to evaluate all the experimental data produced. For instance, only a small part of the CHALMERS data could be modelled; the experiments carried out at 90 °C at FZJ were also not covered. A second objective was to review the published experimental data on RaSO_4 solubility product, in order to verify the reliability of the values currently used in thermodynamic databases.

Extensive Ra uptake experiments were carried out at FZJ at room temperature and 90 °C (see WP2 above), in which 0.5 and 5.0 g/l suspensions of two commercial barite powders (Sachtleben[®] SL and Aldrich[®] AL), were recrystallized in 0.1 M NaCl + 5 μM RaBr_2 solutions. The Ra concentration in the aqueous phase was measured by gamma spectrometry at regular intervals. For the SL barite at 0.5 g/l, a first slow kinetic step was observed, which lasted up to 120-180 days. This was followed by a sudden decrease towards a minimum aqueous Ra concentration, suggesting a fast nucleation of a new $(\text{Ba,Ra})\text{SO}_4$ solid solution phase with ideal or negative interaction parameter ($a_0 \leq 0$). Growth rates of up to 400 μmol m⁻²d⁻¹ were estimated for this step. Thereafter, Ra concentrations in the aqueous solution slowly increased and finally stabilized at the equilibrium line of a regular $(\text{Ba,Ra})\text{SO}_4$ solid solution with the interaction parameter $a_0=1.0$, in agreement with theoretical predictions based on atomistic simulations. These data indicate a non-equilibrium Ra entrapment during the mentioned fast precipitation event, followed by slow recrystallization towards the thermodynamic aqueous - solid solution equilibrium. A similar behaviour was observed for the AL barite; however, the slower decrease in Ra concentration observed with AL barite, in spite of its much larger specific surface area compared to SL barite, was puzzling. X-ray



EUROPEAN
COMMISSION

European
Research Area



diffraction measurements showed nevertheless that SL barite is less crystalline than AL, thus offering an explanation. Apparently, crystallographic defects trigger recrystallization kinetics.

The Ra uptake experiments carried out at CHALMERS and KIT-INE involved lower (picomolar to nanomolar) total Ra concentrations compared to the FZJ experiments (micromolar Ra concentrations). Moreover, in these experiments, ^{133}Ba tracer was added simultaneously to the Ra tracer, allowing an independent determination of $(\text{Ra,Ba})\text{SO}_4$ growth rates. The Ba tracer data indicate for both sets of experiments recrystallization rates and a_0 -values comparable to those inferred from earlier published experiments conducted in a similar range of aqueous Ra concentrations. However, whereas CHALMERS ^{133}Ba data appear to be fully consistent with the classical *heterogeneous* and *homogeneous recrystallization* kinetic models, the KIT-INE data could only be reproduced by applying a newly developed “*continuous recrystallization* model”. This model postulates repeated dissolution-precipitation of previously formed Ra-barite monolayers, whereas the classical models assume a single recrystallization cycle of the initial solid. The different growth mechanism inferred for the KIT-INE experiments may be attributed to the annealing of crystal defects during the long pre-equilibration time (seven months, compared to a maximum of few weeks in the other experiments).

In a specific experiment carried out at CHALMERS, the ^{133}Ba concentration was found to temporarily increase immediately after a second addition of ^{223}Ra to the aqueous solution. This is an indication that the Ra-barite formed after the first ^{223}Ra tracer addition was at least partially dissolved while a new Ra-barite phase was growing. This experiment nicely shows that Ra, even in ultra-trace concentrations, triggers the fast dissolution-reprecipitation of barite towards the aqueous - solid solution equilibrium. For these data, thermodynamic modelling indicates formation of regular $(\text{Ra,Ba})\text{SO}_4$ solid solutions with moderately positive interaction parameters ($a_0 = 0.7\text{-}1.2$), whereas the KIT-INE data point to the formation of solid solutions close to ideality.

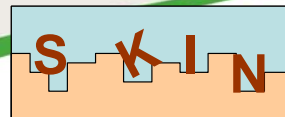
One of the essential results arising from all three mentioned experimental studies is that the dimensionless regular interaction parameter for the binary $(\text{Ba,Ra})\text{SO}_4$ solid solution ranges between $a_0 = 0.0$ and $a_0 \sim 1.0$. The latter value seems to reflect long-term thermodynamic equilibrium and agrees with theoretical predictions based on atomistic simulations. This finding has direct relevance for the safety assessment of radioactive waste repository sites, since it constrains the solubility and thus the mobility of radium in such environments.

The analysis of published data on pure RaSO_4 solubility essentially confirmed that the solubility product, $\log K_s^\circ$ (298 K, 1 bar) = -10.21 ± 0.2 , currently used in reviewed databases



EUROPEAN
COMMISSION

European
Research Area



and in this work, is consistent with the original data and sufficiently accurate to avoid ambiguities in the interpretation of the results obtained within the SKIN project.

Theory on the Affinity Law (Lead S. Ribet, B.Grambow (SUBATECH/ARMINES))

In this study, a review of the data concerning the dissolution or precipitation kinetics of selected minerals (oxides, hydroxides or aluminosilicates) as function of the chemical affinity (i.e. deviation from equilibrium) has been performed. Numerous experimental observations show that the rate decreases when the aqueous solution reaches a composition close to the saturation of the mineral. Investigators have attempted to extrapolate the far-from-equilibrium data to near-equilibrium conditions in order to predict natural processes like weathering, sometimes with poor results because of the lack of understanding of the dependence of dissolution rate on the Gibbs free energy of the reaction.

Kinetic models that attempt to describe variations of the rate when approaching saturation are mostly based upon the transition state theory (TST), which predicts a linear decrease of the rate close to equilibrium. The main hypotheses of the TST applied to solid-water reactions are that the activated complex is the same in the forward rate and backward rate, and that there is only one rate limiting elementary reaction step in the reaction sequence leading to mineral dissolution. The TST-based affinity rate law for mineral dissolution predicts that the rate will become zero at equilibrium, implying that the forward reaction rate (mineral dissolution) remains constant and it is counterbalanced by an equal backward reaction rate (mineral precipitation). This behavior appears valid for some minerals, but for others, the experimental data present a non-linear behavior.

The literature data on the effect of approaching equilibrium on the kinetic of mineral dissolution have been collected and described for about 20 minerals, including simple oxides or hydroxides like brucite, boehmite, gibbsite and quartz; aluminosilicates; natural glasses; and some carbonates. An example of application of the chemical affinity law to the smectite (hydrated aluminosilicate) dissolution is given in Figure 1-10. It demonstrates, in particular, that the dissolution behavior is highly non-linear, and that the fit is not unique.

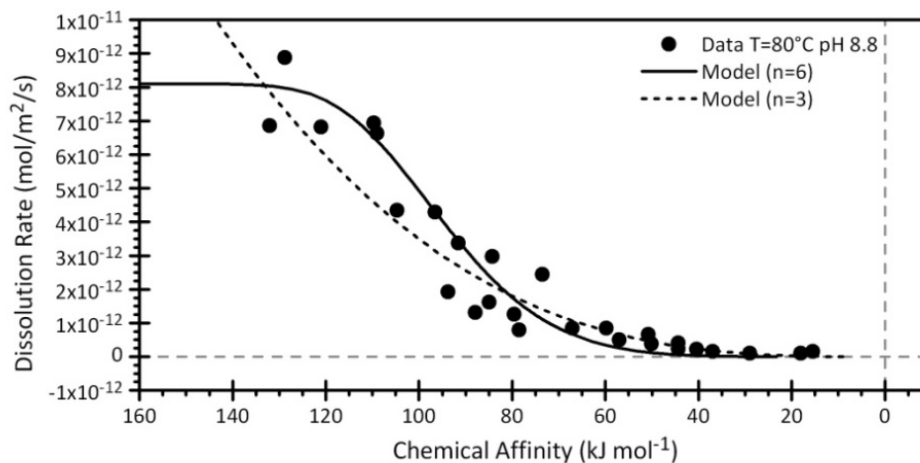
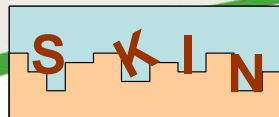


Figure 1-10: Application of the chemical affinity law to smectite dissolution in deionized water at 80°C and pH 8.8. n is the power coefficient at the affinity term in the kinetic rate equation.

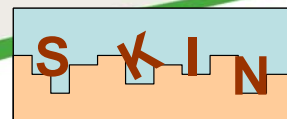
The affinity law could be used to model the kinetics of incorporation of rare earth elements into a mono-layer on sodium/rare earth carbonate minerals as a function of surface to volume ratio and solution concentration of rare earth elements.

We show that although different classes of rate models are available, no generalized rate equation can yet be used to model the mineral dissolution over the full range of geochemical conditions. In some cases, a single TST-based rate law is poorly or not applicable. Moreover, experimental data seem to depend on the history of dissolution of the solid, and on the changes in surface morphology. At conditions very close to equilibrium, the lack of the data and large uncertainties are a real drawback for the study of the impact of saturation state on mineral kinetics. For several minerals, it is still premature to test the affinity law close to equilibrium due to the lack of coherent and precise experimental data.



EUROPEAN
COMMISSION

European
Research Area



1.3.4. Workpackage 5: Synthesis and Safety assessment (Lead: B. Grambow (SUBATECH/ARMINES), L. Duro (AMPHOS 21), K. Spahiu (SKB))

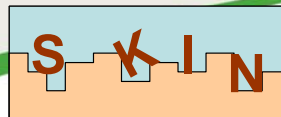
Overall synthesis

The SKIN project has provided a new methodological approach to radionuclide migration in nuclear waste disposal configurations. Indeed, a look only from the solution side, as it is frequently done, is not sufficient: the mineralogical point of view needs to be clearly incorporated into the overall approach, if one wants to assess the role of solid phases in limiting radionuclide migration. Until now, research on radionuclide migration was dominated by short term experiments, yet new observations close to equilibrium are quite different than those far from equilibrium. These new observations include aging of solubility-controlling solid phases; post-sorption processes on the solid influencing the chemical state of the sorbed radionuclides, allowing for in-diffusion or entrapment of trace elements, etc...

The impacts of the results of the SKIN project are expected to be quite different in the near and far field. The near field is characterized by strong chemical gradients and far-from-equilibrium environments, even though local equilibrium/partial equilibrium persists in a global disequilibrium. This leads to the simultaneous and sometimes concurrent action of various dissolution and precipitation reactions, as well as to aging of initial precipitates over periods of many thousands of years. The evolution of the solution composition might lead to re-dissolution of initial precipitates and formation of new precipitates of different composition. Understanding of the temporal evolution of the reaction network is important for quantifying source terms, corrosion processes of containers, evolution of engineered barrier materials interfaces, etc... Of particular interest is the question on how radionuclides behave during these transformations. Typical concepts in safety assessment like “solubility” or “sorption” become quite ambiguous terms under such conditions. In contrast, in the far field, only small phase transformations are expected. But even in this case, some surface modifications and entrapment of radionuclides in solids might occur.

Ageing of initial solids can influence the binding forces of adsorbed material on ageing surface, and recrystallization may lead to entrapment or to changing the structure of adsorbed substance. Close to equilibrium, the dynamics of dissolution and precipitation rates are still only poorly known, including the question of inhibition. Such processes can often only be studied by looking at isotopic exchange, a technique rarely used in migration studies.

The new methodological approach allowed the SKIN project to address a number of important physical/chemical issues related to the safety of nuclear waste disposal, which were long time overlooked in classical safety analyses. In fact, the hypothesis of solid-liquid phase



equilibrium (solubility, sorption) is a key concept in safety assessment. Slow phase transformation, solid state diffusion and incorporation of radionuclides and solid solution formation may occur, which are not yet taken into account in most cases. Neglecting these slow processes close to equilibrium leads mostly to over-conservative assessments. Even if safety margins appear to be large, better knowledge of these margins provides additional confidence. The equilibrium sorption and solubility constraints provide for various repository concepts redundant barriers against safety-relevant release of actinides. A typical solubility value for Am in water at the interface of a nuclear waste glass to clay pore water is 10^{-9} M [1]. Taking for clay rock a typical sorption constant, K_d , of 5000 mL.g^{-1} , and using the measured dispersion coefficient of 0.01, a pore diffusion coefficient of $10^{-10} \text{ m}^2.\text{s}^{-1}$, a clay rock porosity of 20%, a permeability of $10^{-13} \text{ m.s}^{-1}$, and a typical hydraulic gradient of 0.5m.m^{-1} , it is possible to obtain a migration distance across the clay rock after 1000 years beyond 1 m, and a maximum Am concentration $<10^{-29}$ M, well below drinking water standards; for longer times, Am concentrations will disappear due to radioactive decay. If sorbed Am become irreversibly trapped inside the solid phase, it is not anymore available for migration, and actual solution concentrations may be much lower than those calculated. One may argue that it is not necessary to know whether such processes occur, since our calculations show already today that there is no risk for migration to the environment. Nevertheless, better understanding of these slow incorporation processes provides higher confidence in the real safety margins, especially regarding nuclides like ^{79}Se presenting higher solubility and lower sorption than Am.

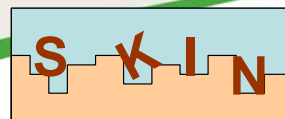
Mechanistic understanding and open questions

One of the key problems was to distinguish thermodynamic and kinetic constraints for enrichment factors of radionuclides at the surface, compared to bulk incorporation, governed for example by surface complexation. The term “equilibrium” does hardly ever apply to the overall system, but only to some sub-systems, hence, we speak of “local” or “partial” equilibrium under conditions of global disequilibrium. For example, even though minerals like calcite or barium sulfate are in solubility equilibrium with the aqueous solution, this is not necessarily true for minor/trace components of the system, such as radionuclides. The example of Radium incorporation in barite has shown that the presence of trace elements like Ra in aqueous solution can lead to a complete recrystallization of the solid under apparent solubility equilibrium. Even if equilibrium is achieved between trace elements in solution and on the solid surface (adsorption equilibrium), there is disequilibrium between the trace element content at the surface and in the bulk of the solid. It is not simple to distinguish incorporation processes from surface layer formation or even from sorption processes. To



EUROPEAN
COMMISSION

European
Research Area



understand and to quantify the underlying mechanism one needs to consider slow kinetics at long experimental times.

The kinetic interpretation of solubility equilibrium may give some insight into the surface incorporation. In studies of isotope exchange on clay surfaces it became obvious that despite the macroscopic equilibrium (“constant Si concentrations in solution”), concurrent dissolution and precipitation proceed, though with equal rates. It is easy to imagine that radionuclides may become embedded in the solid during the precipitation reaction.

Crystallographic distinction between lattice-compatible and incompatible elements alone is not sufficient to assess the potential for radionuclide incorporation in a host mineral. The example of Se(IV) on calcite shows that even for those structurally incompatible elements, incorporation can occur at the surface and in the sub-surface region, leading to enrichments million times higher than in bulk mineral phase. Such entrapment phenomena are strongly dependent on the degree of supersaturation. At present, those phenomena cannot be taken into account in safety assessment because quantification for a disposal site would require the ability to predict supersaturation ratios in the overall evolution of the near field. A detailed study (beyond the scope of SKIN) would be necessary to identify the potential degrees of supersaturation with respect to a large suite of mineral phases at repository-relevant conditions. Under such conditions, one may expect that the geochemical system of natural water in contact with engineered barrier materials and waste matrices will be closer to equilibrium than in laboratory systems. Many literature studies on incorporation of radionuclides in solid host phases are conducted at high degrees of supersaturation; such data may not be relevant to repository conditions.

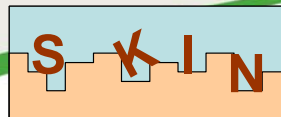
There are also questions concerning the persistence of entrapment with ageing time. For example, the long-term data (>10 yr) for U(VI) sorption on iron hydroxide show a significant modification of the speciation of uranium at the surface with time. Such processes cannot yet be modelled, and the consequences for uranium mobilization can neither be predicted. In this particular case, we do not know whether the retention factors increase or decrease with time. Not only the sorbed substance changes the speciation at the iron oxide surface, but also a recrystallization of the iron oxide with time occurs. Both processes seem to be coupled in a way that the recrystallization leads to a reorganization of adsorbed uranium on the surface.

As far as recrystallisation and uptake mechanisms are concerned, we can distinguish a few kinetic steps and three principal uptake mechanisms (diffusion; overgrowth or surface restructuring; entire recrystallization of the solid) depending on the solid material and the environmental constraints. Yet we do not know, what factors (nucleation/growth pathway? surface free energy?) govern the distinction between the different mechanisms. Figure 1-11



EUROPEAN
COMMISSION

European
Research Area

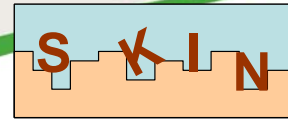


shows two major trends. For the quite different solids studied, we qualitatively obtain close to equilibrium a relation between the rate of dissolution (or surface site detachment) and either (A) the rate of neo-formation of a solid by dissolution/precipitation in case of BaSO₄, deduced from Ra uptake data, showing neo-formation of Ra containing crystals of 10 μm during experimental time or (B) surface restructuring at different degrees: (1) restructuring of many mono-layers in the case of calcite (based on data of ⁴⁵Ca exchange from Curti et al. [2]), (2) restructuring of a single mono-layer in case of alkali rare earth carbonate corresponding to 10⁴ times smaller surface detachment rates in equilibrium than at undersaturated conditions, (3) reaction of only a few surface sites in case of ZrO₂, and (4) absence of any visible reaction of the ThO₂ grain surface with a detachment rate 10⁹ times slower than for calcite, leading to the dominance of detachment from defect sites, grain boundaries, etc.

It appears that dissolution rates of at least 10⁻¹⁵ m·s⁻¹ are necessary to occur during 100 days for surface restructuring beyond a mono-layer. Figure 1-11 illustrates results of the present evaluation in a quantitative manner: data for low reaction rates correspond to solids with very low solubility. Under these conditions and for experiments with powders, the solubility equilibrium is achieved well before a mono-layer becomes exchanged. Surface isotopic exchange rates are then directly proportional to detachment rates. For higher reaction rates, the exchange with a mono-layer occurs fast, but for all solids except BaSO₄, exchange with the sub-surface atomic layers increase only very slowly with increasing reaction rates. In the case of BaSO₄, isotopic exchange seems not to occur on an existing solid phase, but by dissolution of this existing phase and precipitation of a new one. Reasons for this different behavior are not yet known.

We used a reaction progress for 100 days as a reference period, as this corresponds to typical experimental times. If less than a monolayer on the solid phase is involved in the reaction over this time, both reaction modes cannot be distinguished. Dissolution rates are taken from literature [3] (Calcite, hydroxyapatite-HAP, BaSO₄, Quartz, UO₂, ThO₂, ZrO₂) or are obtained by data modelling (NaREE(CO₃)₂ or Illite) in the SKIN project. In the case of illite, dissolution rates are normalized to edge surface areas. The number of monolayers involved in the reaction is obtained from modeling or interpretation of the experimental data: for the rare earth carbonates, data are taken directly from the first order dissolution/precipitation model used in the project to model the uptake of ¹⁵²Eu.

The data in Figure 1-11 show that relevant time scales vary largely: in case of BaSO₄ recrystallisation occurs in relatively short time, but what is the final state in the long term? We followed the evolution of Ra uptake over 2 years, but what about the long term evolution? In case of calcite: some 10 mono layers are involved in isotopic exchange over 100 days, but



how many layers may exchange Ca atoms with the solution in hundreds of years? In case of silicates, less than a monolayer is involved in exchange reactions, even if they are assumed to occur only on edge sites. However, in 10000 years, some incorporation of trace elements in clay minerals may occur well beyond the edge sites.

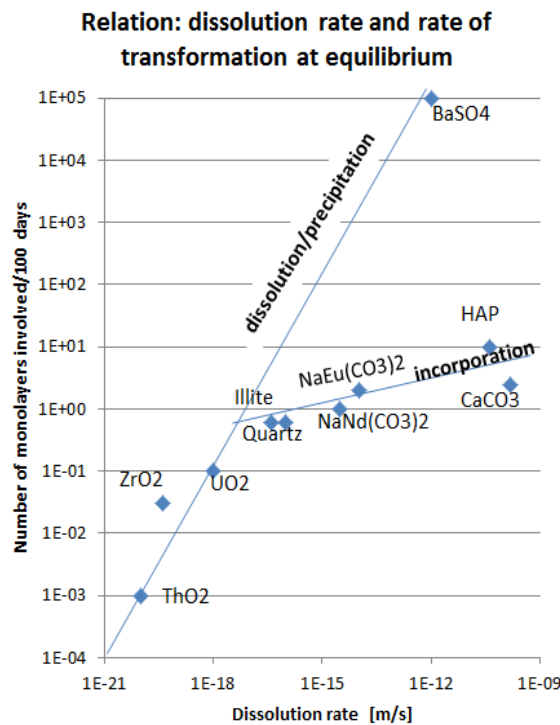


Figure 1-11: Relation between dissolution rates of various solids and the degree of exchange of monolayers at the surface both from literature and from present work. Number of monolayers exchanged for 100 days taken from the data discussed in the text assuming linear extrapolation. The rate data are from James et al. [3]. The value for ThO₂(cr) is obtained directly from the rate data from Hubert et al. [4] at pH 3.1 and the translation of this rate into monolayer exchange rates. In all other cases monolayer exchange rates are obtained from isotopic exchange data. Data for quartz and illite are from [5], for illite the values correspond to exchange rates at edge sites. Data for calcite are from Curti et al. [2]

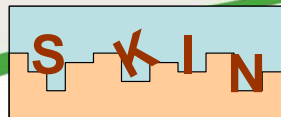
Modelling

In this project, advanced tools were implemented (on the basis of GEM-Selektor code package, <http://gems.web.psi.ch>) for modelling the time-dependent non-equilibrium entrapment of trace radionuclides in solid-solution phases using the principle of partial equilibrium. In particular, the unified uptake kinetics model (UUKM) will ultimately allow modelling of slow kinetic processes even in complex geochemical systems coupled with



EUROPEAN
COMMISSION

European
Research Area



transport of reactive chemical species [6]. The modelling of Ra-barite interaction experiments impressively demonstrated that kinetic effects may well extend over years, before equilibrium conditions are approached. Incorporation of compatible or incompatible trace elements at the surface and/or in the bulk of crystalline phases can now be quantified both at close-to-equilibrium and at far-from-equilibrium conditions. Neglecting such effects in geochemical models of reactive transport is likely to produce biased results. We believe that slow kinetic processes will need to be further explored in the future (both on experimental and modelling sides) in order to provide safer predictions on the fate of radionuclides in geological repository systems.

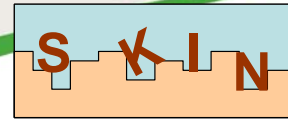
Impact on safety analyses

In general, the experimental data generated in the SKIN project and the models developed show that safety margins in nuclear waste disposal concepts are larger than typically anticipated. Large fractions of transportable radionuclides may become removed from the migration path by partly irreversible entrapment (retention) in the various solid phases along the migration transport path. Impact of uncertainties in solubility values and coupled sorption/solubility processes on radionuclide release from spent nuclear fuel provide new insight into safety margins. Some examples are discussed in the following.

The use of Ra-Ba co-precipitation in safety assessment

In various European spent fuel repository concepts, radium becomes a major dose contributor at long time perspective (after ca. ~300 k years), given the large amounts of ^{238}U disposed off. Solubility constraints for Ra release are important in quantifying dose contributions. The possibility of using its co-precipitation with Ba would be beneficial to safety, because the solubility of Ra in equilibrium with $(\text{Ra,Ba})\text{SO}_4$ is much lower than this calculated with radium sulfate as solubility limiting phase. A scientific debate on the limits of use of formation of a $(\text{Ra,Ba})\text{SO}_4$ solid solution constraints on Ra release in safety assessment is ongoing.

The first use of Ra-Ba co-precipitation in safety assessment was in the Project Opalinus Clay Safety Report /Nagra Technical Report NTB-02-05 (p.145) based on two technical reports [7-8]. Calculations using $\text{RaSO}_4(\text{s})$ as solubility limiting solid phase resulted in Ra concentrations of 4.8×10^{-8} M. In case of co-precipitation, a reduction of Ra concentrations by a factor of 1/5641 to a value of 8.6×10^{-12} M was calculated from the Ra/Ba ratio of 1/5641 in the material balance of the disposal vault, assuming ideal solid solution formation.



Reviewing these calculations, the regulatory body in Switzerland (HSK) pointed to the central role of the temporal evolution. The solid solution model of NAGRA implies that the Ra inventory of the waste is homogeneously distributed in the clay. This is not correct, in particular for the early stages of Ra-release. For this stage the higher solubility of 5×10^{-8} M has to be used. The lower NAGRA value may be more realistic at a later stage but without a detailed kinetic study HSK will use 5×10^{-8} M as a reference value [9].

In the international review organized by OECD-NEA the following comments were made: Except for radium, co-precipitation is not considered. This is conservative, but leads to predictions that significant quantities of some actinides (e.g. ^{230}Th , ^{231}Pa , ^{229}Th) are released into the buffer. This is at variance with experience based on analogy with uranium ores. Co-precipitation is a “reserve FEP” and Nagra should give consideration to incorporating it into models as more data become available [10].

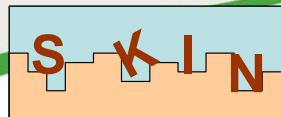
The approach of considering Ra-Ba co-precipitation in the far field considered the presence of Ba in the clay rock and the bentonite was thus criticized because pure $\text{RaSO}_4(\text{s})$ would determine the solubilities inside the damaged canister and this is generally used in the solubility calculations.

In the SR-Site safety assessment [11] the barium present in the spent fuel was considered to co-precipitate with radium, representing an improvement as to the possibility of Ra-Ba-sulfate co-precipitation inside a damaged canister.

Scoping calculations for spent fuel of burn-up 40 MWd/kgU show that Ba and Ra inventories per canister grow with time: Ba reaches a constant level after ~ 500 y and in case of contact with groundwater will precipitate as $\text{BaSO}_4(\text{s})$, while ^{226}Ra reaches its peak after ~ 300000 y after disposal [12].

Two potential scenarios were addressed:

- In case of simultaneous release of Ra with Ba, the former will be readily incorporated into precipitating BaSO_4 to form a $(\text{Ra,Ba})\text{SO}_4$ solid solution. Using a fuel dissolution rate of 10^{-7} /year and a congruent release of Ba, the calculated Ra and Ba concentrations after one year of contact at disposal time 300,000 years (when ^{226}Ra content is largest) are 1.3×10^{-12} M and 4.9×10^{-9} M, respectively. The resulting solid phase has a calculated composition $(\text{Ba}_{0.99942}\text{Ra}_{0.00057})\text{SO}_4$. The dissolved Ra is in the 10^{-11} M range; about 10^3 times lower than from equilibrium with $\text{RaSO}_4(\text{s})$. With the lowest value of sulfate concentration considered (3×10^{-4} M), Ra solubility increases to 7.1×10^{-10} M. Not considering co-precipitation and using $\text{RaSO}_4(\text{s})$ solubility under these conditions results in Ra concentrations are of 1.13×10^{-6} M.



- In the case of fuel dissolution inside a damaged canister, it is considered in SR-Site that the oxidized uranium resulting from fuel dissolution is precipitated as $\text{UO}_2(\text{s})$ on the surface of iron and its corrosion products. When ^{226}Ra is released from a secondary source, like a UO_2 precipitate away from the fuel, there is not sufficient experimental information to establish when and how the system will reach equilibrium with the already precipitated barite resulting from fuel dissolution. In order to obtain further evidence for the co-precipitation kinetics in this case, an experimental study of the barite re-crystallisation and its co-precipitation with Ra was carried out [13]. The experimental investigation of the uptake of ^{226}Ra and ^{133}Ba by two different barite powders (0.31 and $3.2 \text{ m}^2/\text{g}$) in aqueous solutions indicates that there may be a significant uptake of Ra into the bulk of barite crystals. The kinetics of Ra-uptake in barite shows that the uptake rate drops significantly within 400 days, even though a zero exchange rate cannot be unambiguously demonstrated.

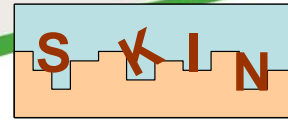
By using larger Ra concentrations and by analysis of the solid phase using ToFs the SKIN project provided a better understanding of the slow re-crystallization towards the thermodynamic aqueous-solid solution equilibrium. For the first time, experimental proof was obtained by direct microanalysis (ToF-SIMS) that Ra is taken up more or less homogeneously in the entire recrystallized solid (not just on the surface), implying that such systems can indeed be treated thermodynamically as solid solutions. The Swedish authorities required various reaction scenarios to be clarified concerning the use of Ra-Ba-sulfate co-precipitation as an argument in safety assessment.

- a) If Ba is released early from spent nuclear fuel and precipitates as secondary phase, can there be redissolution of the precipitates and loss of some of the Ba when Ra-ingrowth reaches a maximum? SKB considers the impact to be weak since diffusive Ba release is very slow and Ra release from secondary UO_2 precipitates is also very slow.
- b) Is it sure that Ba is released proportionally to fuel matrix dissolution, considering that barium zirconates may be present in spent fuel [14-15]. SKB argues that this is only an issue for fuel which has experienced in the reactor at very high temperatures ($> 1500^\circ\text{C}$). Such fuel is not expected in the repository.
- c) Is it possible that Sr is inhibiting uptake of Ra in barite? SKB points to the fact that also (Sr, Ba)-sulfate with high content of Sr can immobilize large amounts of Ra [16-18]. Numerical modeling of $(\text{Ba},\text{Sr},\text{Ra})\text{SO}_4$ indicates that Ra is fixed in the solid phase in the near field of a radioactive waste repository [19] and the Sr present in the waste should not affect considerably the uptake of Ra by barite.



EUROPEAN
COMMISSION

European
Research Area



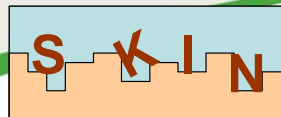
The representation of fuel dissolution in presence of clay slurry in safety assessment

When the buffer is partially or completely eroded, a cavity filled with slurry of water containing colloidal clay particles may exist in the deposition hole. If the canister is breached under such circumstances, the clay particles are not expected to affect the oxidative fuel dissolution rate. Dissolved U(IV) would, however, be expected to sorb strongly to the clay particles. This sorption increases the amount of U(IV) released in solution from the re-precipitated $\text{UO}_2(\text{s})$ or the fuel matrix. In this case, the amount of U(IV) sorbed on clay particles may be calculated as the K_d value for U(IV) on clay particles multiplied by the U(IV) concentration in solution, determined by $\text{UO}_2(\text{s})$ solubility. No limit is posed to the U(IV) release rate from $\text{UO}_2(\text{s})$ to satisfy U(IV) solubility limits in the canister void. In the case when all re-precipitated $\text{UO}_2(\text{s})$ is dissolved due to sorption to clay particles, the remaining U(IV) needed to saturate clay particles is released from the fuel matrix, resulting in an increase of the fuel dissolution rate. To calculate this enhanced U release, the scenario dependent concentration of clay particles and water flow need to be considered. The eroded void volume of the deposition hole is assumed to be filled with clay particles that enhance the dissolution rate of the UO_2 fuel matrix. The void ratio when the transport of bentonite is by colloid dispersion corresponds to a dry density of $37.6 \text{ kg}\cdot\text{m}^{-3}$. This concentration will not be maintained in a large void in the deposition hole, since there will be a concentration gradient from the source of the colloids to the fuel.

If one assumes that a clay slurry with 10 g clay/L enters and leaves the canister with a flow of 100 liters/year, then the total amount of clay is $100 \text{ L/y} * 10 \text{ g/L} = 1000 \text{ g clay/y}$. This amount of slurry will contain at equilibrium an amount of U(IV) sorbed in the clay slurry of $2.5 \cdot 10^{-3} \text{ mol U(IV) per kg clay slurry}$, corresponding to a dissolution rate of $3.4 \cdot 10^{-7}/\text{year}$ -comparable with the average fuel dissolution rate used in SR-Site.

One of the central assumptions in this case is that the concentration of U(IV) in the canister void is equal to the solubility of $\text{UO}_2(\text{s})$ even in the presence of clay particles. If this is not true, clay particles will sorb less U(IV) and the impact of clay on $\text{UO}_2(\text{s})$ dissolution would even be smaller. .

From the result obtained in the SKIN project with $\text{ThO}_2(\text{s})$ as a surrogate for $\text{UO}_2(\text{s})$, it can be concluded that $\text{UO}_2(\text{s})$ dissolution rate is expected to be sufficiently low, so that U(IV) concentrations in the canister void will be lower than the equilibrium value during the residence time of the clay slurry in the canister void. In this case, the amount of U(IV) sorbed on clay particles (proportional to sorption coefficient (K_d) and concentration of U(IV) in solution) will be lower than that in a solution with the U(IV) concentration at UO_2 solubility level.



This is clearly seen from the experimental data, where $[Th]_{(ThO_2+clay)} < [Th]_{(only\ ThO_2)}$. Therefore it can be expected that $[U](t)$ should be lower or much lower than $[U]_{(solubility\ of\ UO_2)}$ in a very long period of time, even longer than the time of clay staying in SNF canister void. Therefore, we may conclude that the invasion of clay slurry to canister void during the glacial period can enhance fuel dissolution, but not as much as conservatively assumed before (Equation 1 [11]), because the U concentration in the canister void is lower than that in clay slurry free conditions.

In any case, the work should be continued in order to better constrain the boundaries and average values of U(IV) to be used for calculating the transport of uranium in the presence of a clay slurry.

Impact of uncertainties in solubility values in safety assessment

High uncertainties in the solubility and sorption of some elements may be reflected in high uncertainties in the results of the calculations used to support safety assessments. The main objective of WP5 of SKIN has been to study the impact of the project in reducing the uncertainty of solubility and sorption data. The evaluation of the impact of new data obtained within SKIN project (together with results of previous studies of literature and field data) is assessed through compartmental modelling. A PA reference case has been defined based on the Swedish SR-Site exercise and calculated with AMBER. Additionally, MC-PhreeqC has been tested as a complementary tool of AMBER to integrate uncertainty analyses.

A simplified system has been calculated where thorium was the only radionuclide considered. The impact of the uncertainty associated with the solubility product of ThO_2 has been assessed. Firstly, a compilation of solubility data of ThO_2 from literature has been performed obtaining a wide range of values depending on the range of pH. That exercise is carried out with PhreeqC and MC-PhreeqC. The obtained output is used as input for the AMBER PA case.

Figure 1-12 shows the results obtained from the MC-PhreeqC model. The relationship between the solubility constant for ThO_2 (x axis), the calculated thorium concentrations in the cell (left axis, red) and the calculated saturation index (right axis, blue) is shown. Only solubility constants below -49.5 (dotted vertical line in Figure 1-12) lead to the precipitation of thorium hydroxide (saturation index = 0 and thorium concentrations below 10^{-10} M) under the flow regimes considered in the calculation. Th concentration becomes dominated by the balance of the dissolution rate and the flow rate when solubility constants are over -49.5, for the flow rate regimes tested.

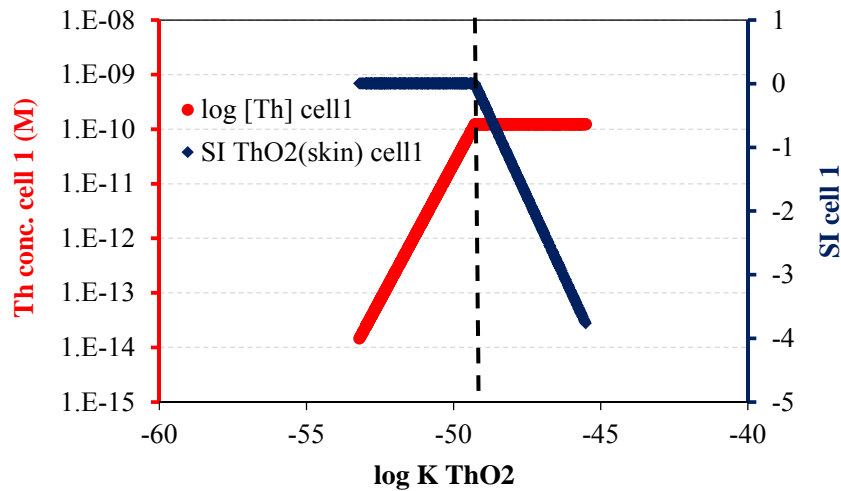
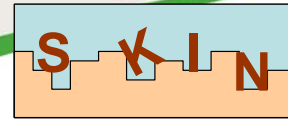


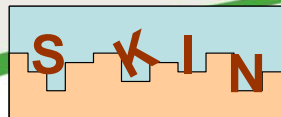
Figure 1-12: Relationship between the solubility constant for thorium hydroxide (“x” axis), the calculated thorium concentrations in the cell (left axis, red) and the calculated saturation index (right axis, blue).

Probability and cumulative distribution functions for Th concentration indicate that, in the 80% of the cases, Th concentration is not limited by solubility limit. The final conclusions would indicate that the concentration of thorium is a steady state value, given mostly by the balance between dissolution rate and flow rate, under the conditions of the simplified system.

Results obtained from the incorporation of MC-PhreeqC output in AMBER show that the concentration is not limited by solubility when the solubility of Th in Bentonite is below around 10^{-11} M.

Future work

Radionuclides from nuclear waste behave in many aspects similar to the non-radioactive isotopes present in the natural environment or to homologue chemical elements. The natural isotopes are involved in the overall geochemical mass transfer processes between various solid and fluid phases. These processes are often ongoing for hundreds of millions of years. How long will take to incorporate the radionuclides from the nuclear waste in the pre-existing geochemical cycle? The SKIN project has opened the door to study such very slow processes close to equilibrium, using the concept of entrapment in mineral solid solutions. However, the link between growth of crystalline solid phases and their capacity for entrapment of trace elements needs to be more clearly established. We are still not capable to quantify the exchange pool of mineral volumes along the transport path and the degree of incorporation of radionuclides from waste in the global exchanges in the mineral-water system. Nevertheless,



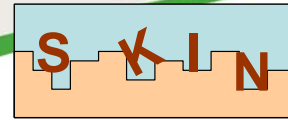
we know that the present sorption models, taking the surface as inert, largely underestimate the available exchange pool, and ignore irreversible uptake. It is, for example, still not possible to quantify ^{41}Ca entrapment in repository rocks with a lot of calcite. The proof of incorporation in some tens to hundreds of monolayers in few hundreds of days exists, but could ^{41}Ca be incorporated within an entire micrometer sized calcite crystal if much longer time would be available, as it was observed in short time for Ra incorporation in BaSO_4 ?

More quantitative approaches need to be developed to assess the magnitude of the safety margins. In this context, an important issue in future work could be the study of entrapment processes in reactive transport models. One needs also to include organics in the assessments.

Finally, a large knowledge base for the significance of entrapment processes in trace element transport is hidden in natural and archaeological analogue systems. It should be possible to use the scientific tools generated in the SKIN project to analyse entrapment processes occurring in natural chemical gradients in a quantitative manner.

Reference

1. Dhanpat Rai, Mikazu Yui, Akira Kitamura (2011). Thermodynamic Approach for Predicting Actinide and Rare Earth Concentrations in Leachates from Radioactive Waste Glasses, Bernd Grambow, *J Solution Chem* 40:1473–1504
2. E. Curti, D. A. Kulik, J. Tits (2005). Solid solutions of trace Eu(III) in calcite: Thermodynamic evaluation of experimental data over a wide range of pH and pCO_2 , *Geochimica et Cosmochimica Acta* 69, 1721.
3. James L. Palandri and Yousif K. Kharaka (2004). A compilation of rate parameters of water-mineral interaction kinetics for application to geochemical modeling, U.S. Geological survey, Open file report 2004-1068, Menlo Park, California
4. Hubert, S., K. Barthelet, B. Fourest, G. Lagarde, N. Dacheux and N. Baglan (2001). Influence of the precursor and the calcination temperature on the dissolution of thorium dioxide *Journal of Nuclear Materials* 297(2): 206-213
5. T. Suzuki-Muresan, J. Vandenberghe, A. Abdelouas, B. Grambow (2011). Solution Control for dissolved silica at 25, 50 and 90°C for quartz, Callovo-Oxfordien claystone, illite and MX80 bentonite, *Phys. Chem. Earth* 36, pp.1648-1660
6. B.M.J. Thien, D.A. Kulik, E. Curti (2013). A unified approach to model uptake kinetics of trace elements in complex aqueous – solid solution systems, *Applied Geochemistry* 41, 135–150.
7. Berner U (2002). Project Opalinus Clay: Radionuclide concentration limits in the near field of a repository for spent fuel and vitrified high level waste, NTB 02-10 (pp. 28-31).

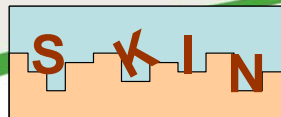


8. Berner U, Curti E (2002). Radium solubilities from SF/HLW wastes using solid solution and co-precipitation models, Paul Scherrer Institute, Villigen, Switzerland, Internal Report TM-44-02-04.
9. HSK 35/99 (2005). Gutachten zum Entsorgungsnachweis der Nagra für abgebrannte Brennelemente, verglastehochaktive sowie langlebige mittelaktive Abfälle (Projekt Opalinuston), Swiss Federal Nuclear Safety Inspectorate, August 2005.
10. International Peer Review of Opalinus Clay PA Project (2004). NEA report 5568, p. 67, OECD
11. SKB (2011). Long-term safety for the final repository for spent nuclear fuel at Forsmark, Main report on the SR-Site project, (Vol. III, p. 664). SKB TR-11-01.
12. Grandia F, Merino J, Bruno J (2008). Assessment of the radium-barium co-precipitation and its potential influence on the solubility of Ra in the near-field. SKB TR-08-07.
13. Bosbach D, Böttle M, Metz V, (2010). Experimental study of Ra^{2+} uptake by barite (BaSO_4). Kinetics of solid solution formation via BaSO_4 dissolution and $\text{Ra}_x\text{Ba}_{1-x}\text{SO}_4$ (re) precipitation. SKB TR-10-43, Svensk Kärnbränslehantering AB.
14. Kleykamp H (1985). The chemical state of the fission products in oxide fuels. Journal of Nuclear Materials, 131, 221-246.
15. Kleykamp H (1993). The solubility of selected fission products in UO_2 and $(\text{U,Pu})\text{O}_2$. Journal of Nuclear Materials, 206, 82-86.
16. Gazineu M H P, Hazin C A, Godoy J M O (2005). Chemical and mineralogical characterization of waste generated in the petroleum industry and its correlation with ^{226}Ra and ^{228}Ra contents. Radioprotection, Suppl. 1, 40, S753-S758.
17. Rodríguez-Galán RM, Carneiro J, Prieto M (2013). Uptake of $\text{Pb}^{2+}(\text{aq})$ by barite-celestite solid-solution crystals. Goldschmidt Conference 2013 Abstracts, 2077.
18. Hedström H, Ramebäck H, Ekberg C (2013). A study of the Arrhenius behavior of the co-precipitation of radium, barium and strontium sulphate. Journal Radioanal. Nucl. Chem. 298, 847–852.
19. Shao H, Dmytrieva SV, Kolditz O, Kulik D, Pfingsten W, Kosakowski G (2009). Modeling reactive transport in non-ideal aqueous–solid solution system. Applied Geochemistry 24, 1287–1300.



EUROPEAN
COMMISSION

European
Research Area



1.4. The potential impact (including the socio-economic impact and the wider societal implications of the project so far) and the main dissemination activities and exploitation of results

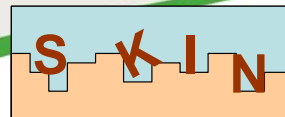
The project SKIN comprises a large number of experimental studies on slow processes close to equilibrium. Understanding of such processes is important in safety analyses of nuclear waste disposal as it influences solubility controls (solid solutions, incorporation etc.) which may influence maximum solution concentrations in groundwaters and associated calculated doses (case of Radium in certain cases).

A number of studies are performed where dynamic exchanges close to solubility equilibrium are followed by isotopic exchange. Examples are ThO_2 , TcO_2 and silicates. Study of exchange rates allow to distinguish whether bulk phases or specific surface sites (grain boundary sites, phases of different degree of crystallinity and hydration state compared to bulk phases...) control solubility.

Radium incorporation from aqueous solution into the crystalline volume of barite (barite in equilibrium with the solution) was studied. The data were explained quantitatively using the GEMS-Selector geochemical code, in a modeling exercise showing the close interaction between different work packages in the project. The temperature dependency of the degree of uptake of Radium followed the temperature dependency of end-member solubility. Detailed spectroscopic studies on radionuclide incorporation in both carbonate and sulfate phases have been performed. Incorporation of trace elements in the bulk volume of a thermodynamically stable pre-existing crystalline phase implies diffusion and/or recrystallization processes, both of which are very slow processes, compared to sorption/desorption processes. In the experimental time frame, the radionuclide uptake by incorporation in the solid is to be considered irreversible. The processes are ongoing for a year or longer.

Sorption/desorption processes are often considered reversible but this is not always the case. A typical example, which in literature is described as irreversible is Cs sorption on illite. Instead of confirming this expected behavior our data on interstratified illite point instead to reversibility. This means that all surface sites allow for dynamic sorption/desorption equilibrium and that for this type of illite there are no sites which allow for incorporation of Cs into the crystalline lattice other than the exchangeable surface sites. This result is surprising and it may be due to the fact that the used interstratified illite blocs Cs diffusion into interlayers.

Even if sorption/desorption is initially reversible slow long term evolution with time due to post-sorption processes might occur. In case of interstratified illite as opposed to pure illite, it



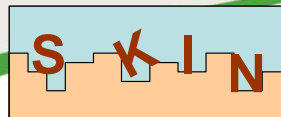
might only be that the diffusion rate is slower than for pure illite, too slow to be experimentally observable. There is another example in the project where such slow transformation rate of initially adsorbed substances is observed in the project after 9 years of aging: the case of adsorption of uranyl ions on ferrihydrite. In fact, both the solid phases and the surface speciation of the radionuclide were modified with time. Current geochemical sorption/ desorption models are not yet able to describe such long term evolutions.

Models for irreversible trace element uptake in host minerals are developed in the project, linking the equilibrium distribution at the surface with the kinetic rates of uptake and (re-)crystallisation. Three existing models of time-dependent trace element uptake in host minerals were evaluated and compared: the Surface (growth) Entrapment Model (SEMO), the Surface Reaction Kinetic Model (SRKM), and the Adsorption-Diffusion-Desorption Model (ADDM). Also a new model was developed, based on the affinity law, applicable for the kinetics of mono-layer incorporation. The models were tested successfully to experimental data and a simplified uptake kinetics model that combines features of SRKM with parameters of SEMO has been implemented in the GEM-Selektor software package.

The temporal evolutions in the solubility and sorption of some elements may be reflected in high uncertainties in the results of the calculations used to support of safety assessments. As a consequence, very conservative model choices have to be done. Reduction of conservatism in the safety assessment has been assessed in the project through a compartmental modeling. A reference case had been defined consisting of a deep geological disposal for spent nuclear fuel in crystalline rock represented by five main compartments: waste, container, bentonite, granite and sink. The calculation results show in which compartments solubility limits are reached.

The project results are expected to impact strongly (1) the use/misuse of solubility data for thermodynamics; (2) the understanding of affinity/rate relations close-to-equilibrium; (3) the inclusion of irreversibility in models on the long-term mobility of radionuclides in geological disposal systems; and (4) the coupling of radionuclide chemistry with main element chemistry in the repository environment. The results of the project show that safety margins in geological disposal concepts are larger than anticipated, but quantification of these margins requires more detailed studies.

The study of SKIN has an important impact in sustaining the scientific methodology in assessing the long-term aspects of radionuclide migration in geological disposal. From the results achieved so far it becomes already clear that a scientific methodology can be developed to quantify the degree of irreversible incorporation of radionuclides in the volume of mineral phases, following initial surface adsorption. Even if this methodology will not be



used directly in performance assessment calculations by nuclear waste management agencies, it will allow quantifying the degree of conservatism if such important beneficial factors for repository safety are ignored, as it is generally the case today.

The research results expected from the SKIN project have a direct impact on the European nuclear power community, including authorities representing public safety concerns. This impact is related to the environmental, economic and political advantages of continued use of the clean and economic nuclear power, as well as its contribution to political stability through lowered dependency of energy import. This is directly related to long term improvement in European competitiveness, employment, environmental quality and quality of life.

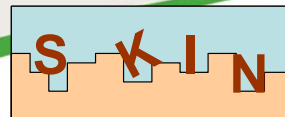
During this project, the results of the research have been successfully disseminated throughout workshops, international conferences and seminars. 24 S&T contributions have been reviewed by End-Users Group and available in the proceedings (Bosbach et al. (2012), Bosbach et al. (2013)). 3 papers with review committee and 1 section book have been published.

A. Proceedings

- Bosbach et al., 2nd Annual Workshop proceedings, 7th EC FP, SKIN
- Bosbach et al., 3rd Annual workshop proceedings, 7th EC FP SKIN

B. Papers

- Grambow B., Montavon G., Abdelouas A., Suzuki-Muresan T., Long-Term Fate and Transport of Fission Products and Actinides in Geosphere (2013) **Mineralogical Magazine**, 77(5) 1206
- Vinograd, V. L., Brandt, F., Rozov, K., Klinkenberg, M., Refson, K., Winkler, B., Bosbach, D., Solid–aqueous equilibrium in the $BaSO_4$ – $RaSO_4$ – H_2O system: First-principles calculations and a thermodynamic assessment (2013) **GCA** 122, 398 - 417
- Thien B.M.J., Kulik D.A., Curti E. (2013) A unified approach to model uptake kinetics of trace elements in complex aqueous – solid solution systems, **Applied Geochemistry** 41, Pages 135–150
- Thien B.M.J., Kulik D.A., Curti E. (2013) Modeling trace element uptake kinetics in secondary minerals. **Procedia Earth and Planetary Science** 7, 838-841
- Zheng Z., Kang M., Wang C., Liu C., Grambow B., Duro L., Suzuki-Muresan T. (2014) Influence of gamma irradiation on uranium determination with arsenazo III in the presence of Fe(II)/Fe(III), **Chemosphere**, in press



C. Section in a book

- Brandt, F., Klinkenberg, M., Breuer, U., Rozov, K., Bosbach, D., Recrystallization of Barite in the presence of Radium (2013) **Energie & Umwelt / Energy & Environment** 197

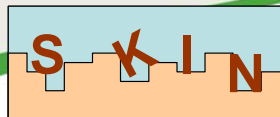
D. Oral presentations

- Suzuki-Muresan T., Vandenborre J., Grambow B., Thorium oxide solubility behavior vs. the surface crystalline state (2014) REDUPP Conference, Stockholm, Sweden
- Brandt F., Klinkenberg M., Vinograd V., Rozov K., Bosbach D., Radium solubility in the presence of barite: sorption experiments and atomistic modeling (2013) Migration'13 Conference, Brighton, UK
- Brandt F., Klinkenberg M., Vinograd V., Rozov K., Bosbach D., Solid solution formation and uptake of Radium in the presence of barite (2013) Goldschmidt'2013 Conference Florence, Italy
- Brandt F., Klinkenberg M., Vinograd V., Rozov K., Bosbach D., Radium solubility control in the $BaSO_4 - RaSO_4$ solid-solution aqueous solution system (2013) Darmstadt, Germany
- Brandt F., Klinkenberg M., Vinograd V., Rozov K., Bosbach D., Recrystallization of barite in the presence of Radium – a microscopic and spectroscopic study (2013) Migration'13, Brighton, UK
- Klinkenberg M., Brandt F., Breuer U., Bosbach D., A Microscopic and ToF-SIMS Study on the Ra Uptake by barite (2013) Goldschmidt'2013 Conference Florence, Italy
- Kulik D.A., Thien B., Curti E., Modeling Trace Element Uptake Kinetics in Secondary Minerals (2013) Water-Rock Interaction Conference, Avignon, France
- Suzuki-Muresan T., SKIN: Investigation of slow processes in close-to-equilibrium conditions in water/solid systems and their impact on the mobility of radionuclides in radioactive waste geological repositories (2013) Euradwaste Conference, Vilnius, Lithuania
- Suzuki-Muresan T., Vandenborre J., Grambow B., Valls A., Duro L., Evaluation of discrepancies in tetravalent oxide solubility values by isotopic exchange and its impact on the safety assessment (2013) Migration'13 Conference, Brighton, UK
- Kulik D.A., Thien B., Curti E., Partial-equilibrium concepts to model trace element uptake (2012) Goldschmidt'2012 Conference, Montreal, Canada



EUROPEAN
COMMISSION

European
Research Area



- Thien B., Kulik D.A., Curti E., Adding uptake kinetics and surface entrapment to geochemical models (2012) Goldschmidt'2012 Conference, Montreal, Canada

E. Posters

- Brandt, F., Klinkenberg, M., Breuer, U., Rozov, K., Bosbach, D., Uptake of Radium during Barite Recrystallization (2013) Euradwaste Conference, Vilnius, Lithuania
- Thien B., Heberling F., Kulik D.A., Modeling Non-Equilibrium Uptake of Se(IV) Upon Calcite Precipitation (2013) Goldschmidt'2013 Conference, Florence, Italy
- Thien B., Kulik D.A., Curti E., Kinetics of trace element retention in minerals: Comparison of modelling approaches (2012) Workshop, Univ. Oviedo, Spain



EUROPEAN
COMMISSION

European
Research Area

